Mineralogical Magazine, June 2018, Vol. 82(3), pp. 625–647

Platinum-group element and gold contents of arsenide and sulfarsenide minerals associated with Ni and Au deposits in Archean greenstone belts

MARGAUX LE VAILLANT[1,2,*], STEPHEN J. BARNES[1], MARCO L. FIORENTINI[2], SARAH-JANE BARNES[3], ADAM BATH[1] AND JOHN MILLER[1,2]

[1] CSIRO / Mineral Resources, Kensington, Perth, Australia
[2] Centre for Exploration Targeting, School of Earth Sciences and ARC Centre of Excellence for Core to Crust Fluid Systems, University of Western Australia, Perth, Australia
[3] Département des sciences appliquées, Université du Québec a Chicoutimi (UQAC), Québec, Canada

[*Received 31 August 2017; Accepted 17 December 2017; Associate Editor: Iain McDonald*]

ABSTRACT

Post-magmatic alteration of certain magmatic Ni sulfide ores in Western Australia, the Miitel deposit and the Sarah's Find prospect, produced Ni–As–PGE haloes around massive sulfides. A study of the composition of arsenide grains from these hydrothermal haloes, along with arsenides from various magmatic and hydrothermal mineralized environments in other localities, was conducted in order to compare their composition, and assess their potential use as indicator minerals for exploration vectoring, as well as to gain knowledge on their crystallization history. Concentrations in trace elements such as platinum-group elements (PGEs), Au and other metals was obtained by laser ablation inductively coupled plasma mass spectroscopy analyses. Results show that variations in PGEs and Au compositions can be related to the magmatic *vs.* hydrothermal origin of the grains; and to their provenance from deposits enriched in either Ni, Au or both. Magmatic NiCoFe sulfarsenides have strongly correlated, high IPGE (Os, Ir, Ru, Rh) contents up to 100 ppm Ir, compared with maximum values in hydrothermal sulfarsenides of ~1 ppm. Gold in hydrothermal sulfarsenides from Au-mineralized ultramafic rocks extends up to 500 ppm, with typical values of 3–30 ppm; similar values are also found in nickeline (also called niccolite). These results suggest that nickel arsenides could potentially be used as indicator minerals for nickel and gold exploration. Trace-element contents of arsenide grains in shear zones could be used to deduce the presence of Ni or Au mineralization upstream in the fluid pathway.

KEYWORDS: platinum-group element, gold, nickel arsenide, sulfarsenide, Archean greenstone belts.

Introduction

TRACE-element composition, specifically precious metal compositions, of certain minerals associated with ore deposits can provide valuable information on their genetic history, and that of the mineralized system they are related to, e.g. PGE contents of oxide and sulfide minerals in Ni sulfide ore systems (Locmelis *et al.*, 2013, Dare *et al.*, 2010*a*,*b*, 2011; Godel *et al.*, 2012). This study presents the results of laser ablation inductively coupled plasma mass spectrometry (LA-ICP-MS) analyses collected on a set of nickel-cobalt arsenides and sulfarsenides of different paragenesis (magmatic *vs.* hydrothermal), and associated with different types of mineralized systems (gold *vs.* nickel). In the following discussion we refer to all the arsenide and sulfarsenide minerals studied as 'arsenides' for brevity. The trace-element concentrations in

*E-mail: Margaux.levaillant@csiro.au
https://doi.org/10.1180/minmag.2017.081.100

This paper is published as part of a thematic set in memory of Professor Hazel M. Prichard

platinum-group elements (PGEs), gold and metals of these grains reflect this origin and spatial association. Arsenic-rich minerals, including gersdorffite (NiAsS), nickeline (also called niccolite NiAs), cobaltite (CoAsS) and arsenopyrite (FeAsS) from five different localities within the Kalgoorlie Terrane of the Western Australian Yilgarn Craton were studied (Fig. 1): Two magmatic nickel sulfide deposits that are poor in gold, the Miitel deposit and the Sarah's Find prospect, and that have undergone an episode of As-rich hydrothermal alteration, interpreted as being related to an orogenic gold event that overprinted them (Le Vaillant *et al.*, 2015, 2016*b*); one magmatic nickel sulfide deposit that has been overprinted by orogenic As-Au-rich fluids producing economic gold mineralization, the Mariners deposit (Goodgame, 1997); one magmatic nickel sulfide deposit that has not been affected by As-rich alteration, the Perseverance deposit (Barnes *et al.*, 2011; Diragitch, 2014); and one gold deposit in ultramafic rocks lacking magmatic sulfides, the Wattle Dam gold deposit (Walshe *et al.*, 2014).

In this study, arsenide occurrences are separated into different categories reflecting their origin and spatial association (Fig. 2). Two different categories are used: (1) magmatic arsenides and (2) hydrothermal arsenides. We use the term (1) magmatic arsenides to define nickel arsenides that crystallize within the nickel massive sulfides upon cooling of the host intrusion or magma flow. Arsenic is an element which is present only in ultra-trace proportions in mafic-ultramafic magmas forming the ore deposits (Helmy *et al.*, 2013*b*; Canali *et al.*, 2017), but which is enriched in the crust, particularly in sedimentary units (Ketris and Yudovich, 2009; Samalens *et al.*, 2016). Enrichment of the magma in arsenic is produced by thermomechanical erosion of crustal rocks and contamination of the magma upon intrusion or eruption. If arsenic has been added to the magma, and sulfide liquid segregation occurs (the essential necessary step to the genesis of magmatic nickel sulfide mineralization), arsenic will tend to be concentrated in the liquid sulfide droplets, along with the other chalcophile elements (Helmy *et al.*, 2010).

As the sulfide liquids crystallizes, arsenides will then crystallize alongside the Fe–Ni–Cu sulfide minerals, either as a liquidus phase directly from the melt where As concentrations are exceptionally high (Bai *et al.*, 2017), or otherwise as part of late residual assemblages close to the solidus (Helmy *et al.*, 2010), or in some unusual cases from a discrete immiscible arsenide liquid phase (Hanley, 2007*b*; Godel *et al.*, 2012*b*; Pina *et al.*, 2015). We use the term 'hydrothermal arsenides' to define arsenides that form by overprinting of the mineralized magmatic system by As-rich hydrothermal fluids. The arsenides in this setting form well after Fe–Ni–Cu sulfides have crystallized and the magmatic system has cooled down, as a result of the interaction between As-rich fluids and solid ores (Le Vaillant *et al.*, 2015, 2016*a*,*b*). In addition, we also present data on 'hydrothermal' arsenides formed in non-magmatic Au-bearing hydrothermal vein systems. For the purpose of this study, we compiled a set of representative samples for these two types of arsenides (magmatic *vs.* hydrothermal), collected at different localities displaying the presence of either nickel sulfide mineralization, gold mineralization or in one case both (Fig. 2).

Background

Occurrence of nickel arsenides

Magmatic arsenides that evidently crystallized directly from sulfide or associated arsenide melt have been described in the following studies: at the Carratrace and the Arroyo de la Cueva deposits in Spain (Hem *et al.*, 2001), Beni Bousera in Morocco (Gervilla *et al.*, 1996; Pina *et al.*, 2013), the Ni-Cu deposit at Las Aguilas in Argentina (Gervilla *et al.*, 1997), Serrania de Ronda in Spain (Pina *et al.*, 2015), the Copper Cliff North Area, Dundonald Beach South and Creighton Ni-Cu-PGE deposits in Canada (Szentpeteri *et al.*, 2002; Hanley, 2007; Dare *et al.*, 2010*a*), and the Rosie nickel prospect and the Spotted Quoll deposits in Western Australia (Godel *et al.*, 2012; Prichard *et al.*, 2013). Only a small portion of these studies present the results of LA-ICP-MS analyses on arsenides, but the few that do all agree that magmatic Ni-Co arsenides contain elevated concentrations of PGEs. Arsenides acted as collectors for the PGEs, particularly Pd and Pt, with an average concentration of 257 ppm Pd, 536 ppm Pt at the Rosie prospect (Western Australia, Godel *et al.* (2012), 234 ppm Pd, 83 ppm Pt at the Spotted Quoll nickel deposit (Western Australia; Prichard *et al.*, 2013), and 52 ppm Pd, 167 ppm Pt at the Dundonald Beach nickel deposit, Canada (Hanley, 2007). Gold concentration of these magmatic arsenides vary widely between different deposits, ranging from an average of 0.11 ppm Au at Spotted Quoll (Prichard *et al.*, 2013) to 0.708 ppm Au at Rosie (Godel *et al.*, 2012).

https://doi.org/10.1180/minmag.2017.081.100 Published online by Cambridge University Press

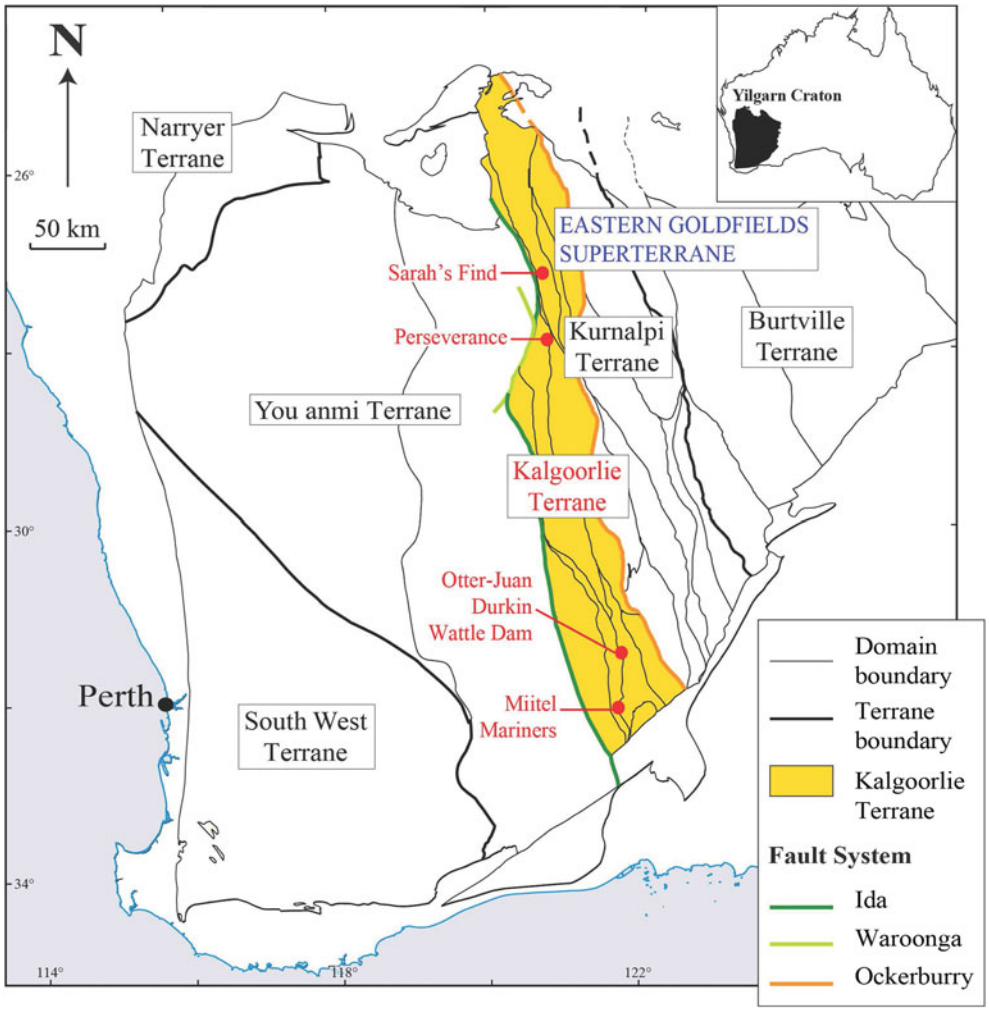

FIG. 1. Simplified geological map of the Yilgarn Craton showing the location of the case studies, modified from (Cassidy *et al.*, 2006).

A few occurrences of nickel arsenides within magmatic nickel sulfide deposits have been interpreted as hydrothermal remobilization of primary, late magmatic arsenide-rich ores, such as the Kylmäkoski Ni–Cu deposit in Finland (Gervilla *et al.*, 1998), or the Ni–Cu–PGE sulfide ores of the komatiite-hosted Fortaleza de Minas deposit in Brazil (De Almeida *et al.*, 2007). Additionally, a few deposits are interpreted as being entirely the product of As-rich hydrothermal fluids that leached Ni, Co, PGE and sometimes Au from adjacent rocks or massive sulfides and redeposited them as Co–Ni–PGE arsenide ores, such as the Cobalt deposit in Canada (Sampson and Hriskevich, 1957; Goodz, 1986), the Bou Azzer deposit in Morocco (Leblanc and Fisher, 1990; Ahmed *et al.*, 2009), or the Cu–Ni–Co–As (U) mineralization in the Anarak area in central Iran (Bagheri *et al.*, 2007). Minor Ni arsenides have also been reported from the Avebury hydrothermal Ni deposit in Tasmania, although the As content of this orebody is very low (Keays and Jowitt, 2013). No trace-element concentrations have been reported on these purely hydrothermal nickel arsenides.

Arsenide minerals, mainly arsenopyrite, but also Ni-Co arsenides such as cobaltite and nickeline, are often present in gold mineralized systems. However, few studies have looked at their

https://doi.org/10.1180/minmag.2017.081.100 Published online by Cambridge University Press

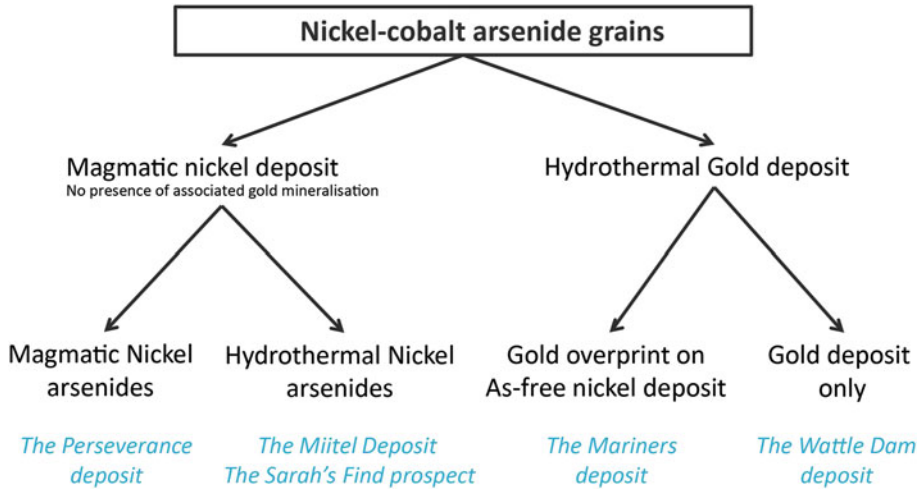

FIG. 2. Classification diagram of the different 'arsenide types' present within the case studies used for this project.

trace-element compositions using LA-ICP-MS. Numerous studies report gold concentrations in arsenopyrite, which vary a lot within as well as between deposits, probably due to complex redistribution processes and to the fact that gold in arsenopyrite, also called 'invisible gold' (Cook and Chryssoulis, 1990), is often present as nanoparticles (<250 nm) with a heterogeneous distribution. A study by Deol *et al.* (2012) on arsenopyrites from the Bhukia-jagpura gold prospect in southern Rajasthan, India, reported Au concentrations varying between 6 and 10 ppm Au, and very low Pt values (mostly below detection) with an average of 40 ppb Pt (other PGEs not reported). Another study by Cook *et al.* (2013) on arsenopyrite from a Proterozoic orogenic gold deposit, Tanami gold province, north-central Australia, reported gold values between 8 and 338 ppm Au, but no PGE data were presented. At this stage, there are no available published data on arsenide minerals from settings entirely devoid of economic mineralization.

Platinum-group elements in arsenide minerals

It is well established that the PGEs have strong geochemical affinities for As. Platinum, Ir, Os and Ru have a strong propensity to make PGE-arsenide minerals under a range of conditions, including under some circumstances through direct precipitation from sulfide magmas (Helmy *et al.*, 2013*a*; Canali *et al.*, 2017; Bai *et al.*, 2017) and silicate magmas (Barnes *et al.*, 2016). The magmatic partitioning of PGEs between solid Fe–Ni sulfide, arsenide melts and sulfide melt has been studied experimentally (Helmy *et al.*, 2010, 2013*b*). However, their tendency to partition into Ni-Co-Fe arsenides and sulfarsenides is less well known and relatively few experimental datasets are available.

Geology of the study sites

The Perseverance deposit: example of a nickel deposit containing magmatic arsenides

The Perseverance nickel sulfide deposit (Barnes *et al.*, 1988*a*,*b*, 2011; Perring 2015) is located in the Archaean Kalgoorlie Terrane, within the Eastern Goldfields Superterrane (Cassidy *et al.*, 2006) (Fig. 1). Perseverance, previously known as Agnew (Barnes *et al.*, 1988*b*), is one of the largest known komatiite-hosted nickel-sulfide deposits. It comprises a large tonnage of matrix ore with variably tectonized massive sulfides, representing pre-mining resources of 31,300 kt at 5.9 wt.% Ni, at tenors averaging 9 wt.% Ni (Barnes *et al.*, 1988*b*). The ore is composed of both matrix and disseminated (15–45 vol.%) sulfides with 1–2 wt.% Ni (pyrrhotite, pentlandite, minor chalcopyrite, pyrite and traces of gersdorffite) and massive sulfides with 7.5–9 wt.% Ni (80 vol.% pyrrhotite, <8 vol.% pentlandite and <12 vol.% pyrite, chalcopyrite and magnetite). The longest massive sulfide shoot at Perseverance is the 1A ore shoot, extending as variably mylonitized breccia ore entirely within felsic footwall rocks, up to 100 m

https://doi.org/10.1180/minmag.2017.081.100 Published online by Cambridge University Press

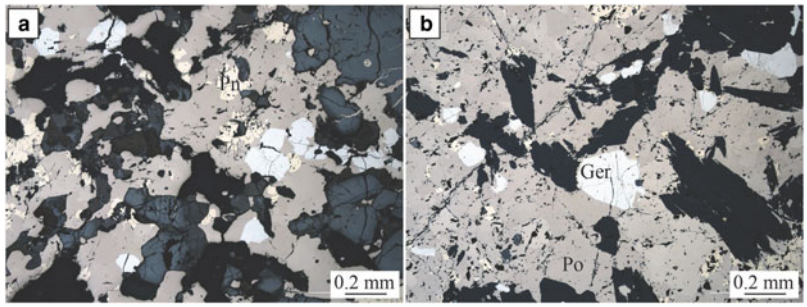

FIG. 3. Perseverance. Photomicrographs in reflected light of massive sulfides from the Perseverance nickel deposit. Ger = gersdorffite, Pn = pentlandite and Po = pyrrhotite.

north of the disseminated sulfide body. Massive sulfides from the 1A ore shoot are locally enriched in arsenic (Fig. 3). Arsenides within this ore shoot, mainly gersdorffite, were sampled for this study.

The Miitel deposit and the Sarah's Find prospect: magmatic nickel deposits containing hydrothermal arsenides

The Miitel deposit is an Archean komatiite-hosted Ni–Cu–PGE deposit located on the eastern flank of the Widgiemooltha Dome (Seat *et al*., 2004) within the Kalgoorlie Terrane (Swager, 1997) (Fig. 1). The Miitel ore bodies are located at the basal contact between the Widgiemooltha komatiites and the Mount Edwards basalt; the whole area has undergone upper greenschist- to lower amphibolite-facies metamorphism (McQueen, 1981, 1987; Hayward, 1988; Barnes and Hill, 2000; Le Vaillant *et al.*, 2015; Moroni *et al.*, 2017; Caruso *et al.*, 2017). Le Vaillant *et al*. (2015) documented a cryptic Ni-As-Pd-Pt geochemical halo around the ore body, formed by the late magmatic or metamorphic circulation of arsenic-rich hydrothermal fluids (Fig. 4). These As-rich fluids were prevalently flowing upwards, mainly along the footwall contact between the komatiitic host rock and the footwall basalt, and along late SSW shallow-dipping cross-cutting splay structures. These hydrothermal fluids collected Ni and PGEs, mainly Pd and Pt, from the massive nickel sulfides, transported them, and re-deposited them within mm to cm wide quartz and/or carbonate veins close to the footwall contact.

The geochemical halo produced by the hydrothermal circulation of As-rich fluids extends along the basal contact at least 250 m away from the ore. In addition, it is inferred that the larger spread of As-rich metasomatism in rocks surrounding the deposit (As > 100 ppm in whole-rock data), especially along the splay structures outside the limit of drilling availability, could reflect an even wider Ni–As–PGE halo. At Miitel, arsenic seems to have played the critical role of a ligand in remobilizing Ni and PGEs and redepositing them as nickel arsenides within a geochemical halo (Le Vaillant *et al.*, 2015). These late, arsenic-rich fluids are commonly related to orogenic gold events (Eilu and Groves, 2001). The As-rich fluids at Miitel produced two distinct modes of occurrence of arsenides: (1) gersdorffite crystallized *in situ* by local alteration of the massive sulfides (Fig. 5); and (2) gersdorffite that precipitated in small quartz-carbonate veins away from the massive sulfides (Fig. 6) (remobilization of the metals and PGE from the massive sulfides into the hydrothermal fluids). Both types were analysed by LA-ICP-MS within this study.

The Sarah's Find prospect is located 4.5 km north of the Mount Keith deposit, in the Agnew-Wiluna greenstone belt (Fiorentini *et al.*, 2007) (Fig. 1). It is composed of very small lenses or stringers of massive sulfides at the basal contact between the Mount Keith komatiite and the Mount Keith dacite footwall. At Sarah's Find, a Ni–Co–Pd–As geochemical halo was also observed around the massive sulfides (Le Vaillant *et al.*, 2016*b*), as shown in Fig. 7. This halo is interpreted as the result of combined physical (solid state) and hydrothermal remobilization of Ni, Co and PGEs (Pd, Pt) from the massive sulfides. Physical remobilization, in the form of arsenide minerals smeared along shear planes within a prominent mineral lineation, is observed up to 100–150 m away from the massive sulfides, within the footwall dacite, along the contact with the komatiitic host rock (Mount

https://doi.org/10.1180/minmag.2017.081.100 Published online by Cambridge University Press

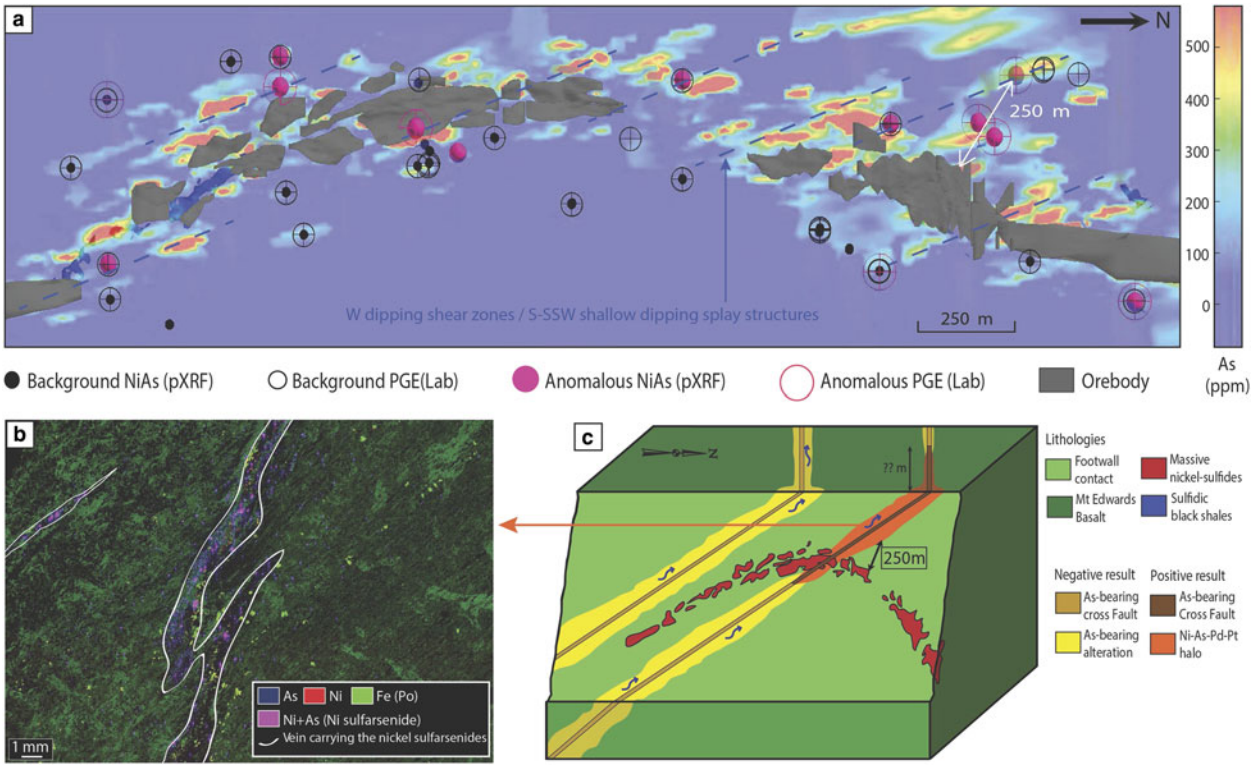

FIG. 4. Summary of results from the study of the Miitel deposit, modified from Le Vaillant *et al.* (2015). (*a*) Perspective view from gOcad® of a long section through the 3D model of the Miitel deposit. This image combines: (1) distribution of the arsenic in mg/g at the contact between the basalt and the komatiites (model derived using Leapfrog®); (2) location of pXRF analyses showing anomalously high Ni and As concentrations; and (3) location of laboratory PGE analyses highlighting samples enriched in PGE. (*b*) False colour element concentration map (As blue, Ni red, Fe green), of samples DRD918-358.6 which contains nickel arsenides within small hydrothermal quartz and/or carbonate veins cross cutting the Mount Edwards footwall basalt. This map was produced using the data collected with the Maia detector array on the X-ray fluorescence microscopy beamline, at the Australian Synchrotron in Melbourne. (*c*) 3D block model of the Miitel system showing the possible application of the Ni–As–Pd geochemical halo to exploration targeting for nickel sulfides.

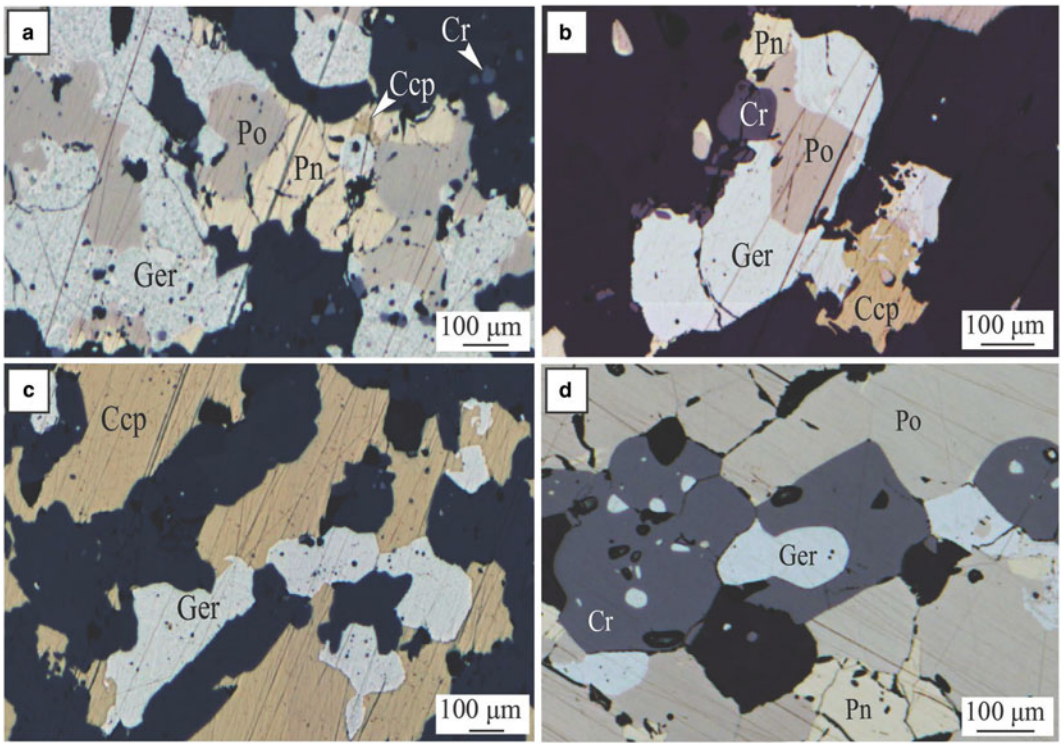

FIG. 5. Miitel. Photomicrographs showing arsenides present within the massive sulfides due to alteration by As-rich hydrothermal fluids. (*a*), (*b*) and (*c*) photomicrographs in reflected light of sample DRD738-371.44, area of the massive sulfides enriched in chalcopyrite and gersdorffite; embayment of gersdorffite in chalcopyrite and pyrrhotite (*c*), intergrain infill (*a*) and intergrain infill, mantling and breakdown of pyrrhotite grains into gersdorffite (*b*). (*d*) Photomicrographs in reflected light of sample DRD738-371.51, massive sulfides enriched in gersdorffite. Ccp = chalcopyrite, Cr = chromite, Ger = gersdorffite, Pn = pentlandite and Po = pyrrhotite. Adapted from Le Vaillant *et al.*, 2015.

Keith Ultramafic Unit), parallel to the direction of shearing. Nickel, Co and PGEs (mainly Pd and to a lesser degree Pt) are also interpreted as being hydrothermally remobilized by syn-deformation As-rich hydrothermal fluids, and re-deposited in an even larger halo than the one produced by physical remobilization, prevalently along the direction of shearing. These As-rich fluids collected Ni, Co and Pd from the Sarah's Find massive sulfides and re-deposited them as nickel sulfarsenides within the sheared footwall dacite, along the dominant NNW striking foliation, creating this geochemical halo extending along the direction of shearing up to 1780 m away from the massive sulfides.

Two types of nickel arsenides associated with this physical and hydrothermal halo were observed. Type (1) is interpreted as forming by purely hydrothermal remobilization of Ni–Co–Pt–Pd from the massive sulfides by As-rich fluids re-depositing them as Co-rich gersdorffite (NiAsS) within the foliation both within the ultramafic host rock and within the dacite footwall (Fig. 8*d*,*e*,*f*). Type (2) is composed of Ni-rich gersdorffites formed by hydrothermal alteration of the mechanically sheared sulfides by As-rich hydrothermal fluids. The trace-element compositions of both types of arsenides were measured as part of this study.

The Wattle Dam gold deposit: Ni-poor hydrothermal gold deposit

The Wattle Dam orogenic lode gold deposit is located ~25 km south-west of Kambalda (Fig. 1) and occurs within the >250 Moz Au Kalgoorlie Terrane (Goldfarb *et al.*, 2005) along the NNW-

https://doi.org/10.1180/minmag.2017.081.100 Published online by Cambridge University Press

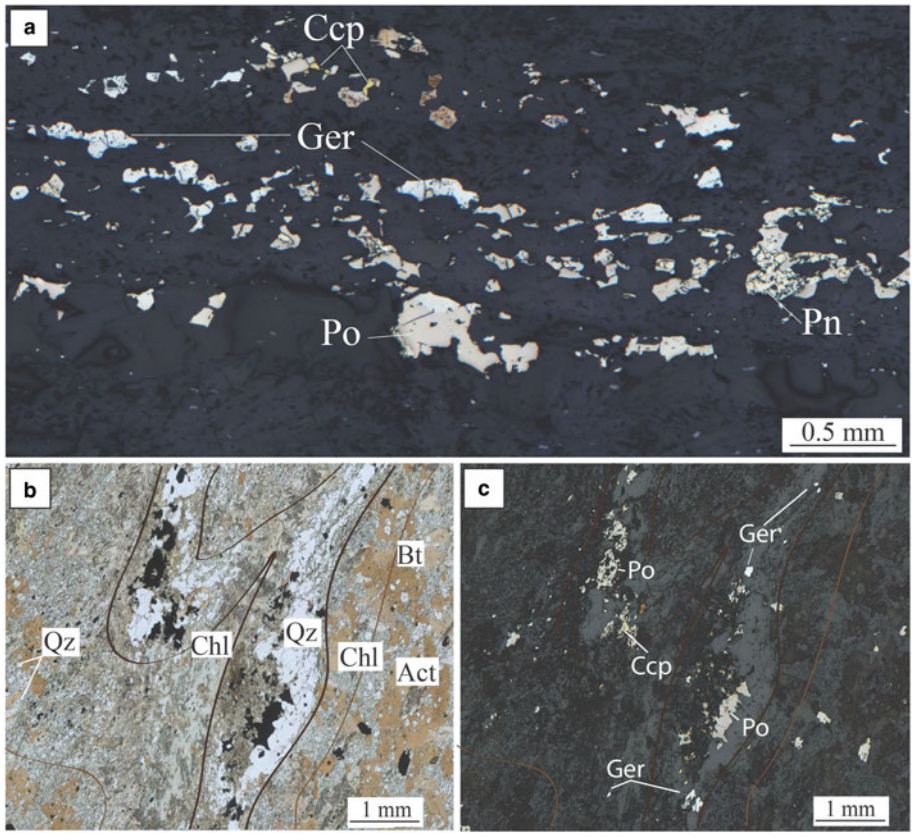

FIG. 6. Miitel. Photomicrographs showing hydrothermal arsenides in the hydrothermal haloe. (*a*) Photomicrograph in reflected light of sample DRD738-366.23, (*b*) and (*c*) photomicrographs in transmitted and reflected light of sample DRD912-239.5. Photos show the presence of quartz veins cross cutting the Mount Edwards basal footwall assemblage of actinolite/tremolite +/– biotite, and containing nickel arsenides (gersdorffite) with pyrrhotite and minor chalcopyrite, associated with green hornblende, cross cutting the Mt Edward basalt. Act = actinolite, Bt = biotite, Ccp = chalcopyrite, Chl = chlorite, Ger = gersdorffite, Pn = pentlandite, Po = pyrrhotite and Qz = quartz. Adapted from Le Vaillant *et al.* (2015).

striking Spargoville Shear. The Wattle Dam deposit is located within the fault bounded Hampton Komatiite from the Coolgardie Domain. The komatiite dips sub-vertically and is locally intruded by granitoids to the east and fault bound by basalts high in magnesium and meta-sediments to the west. The main gold shoot plunges steeply towards the north (~70°) and is predominantly hosted by intense biotite-amphibole altered komatiite with thin (1 m) interflow shale that occurs within the main lode (Hutchison, 2011). Mineralization is considered to have formed at ~2650 to 2645 Ma.

The main lode is a high-grade (average 20 g/t Au) body that is <50 metres in strike and 12 metres in horizontal width. It extends to a depth of >300 metres. Veins of gold cross-cut biotite-amphibole altered and deformed komatiites and interflow shale. Gold also occurs as nuggets up to cm size within the biotite-amphibole assemblage as well as in carbonate veins (Hutchison, 2011; Cloutier *et al.*, 2011; 2012) and as inclusions in arsenides near the main lode (Fig. 9). Arsenides with gold inclusions are used here in this study on trace-element composition.

Details on the various alteration stages and associated paragenesis are presented in Walshe *et al.* (2014). They describe three main stages of metasomatism: stage 1 biotite-amphibole alteration, which is cross cut by stage 2 alteration, which is divided into three sub-stages. One of these

https://doi.org/10.1180/minmag.2017.081.100 Published online by Cambridge University Press

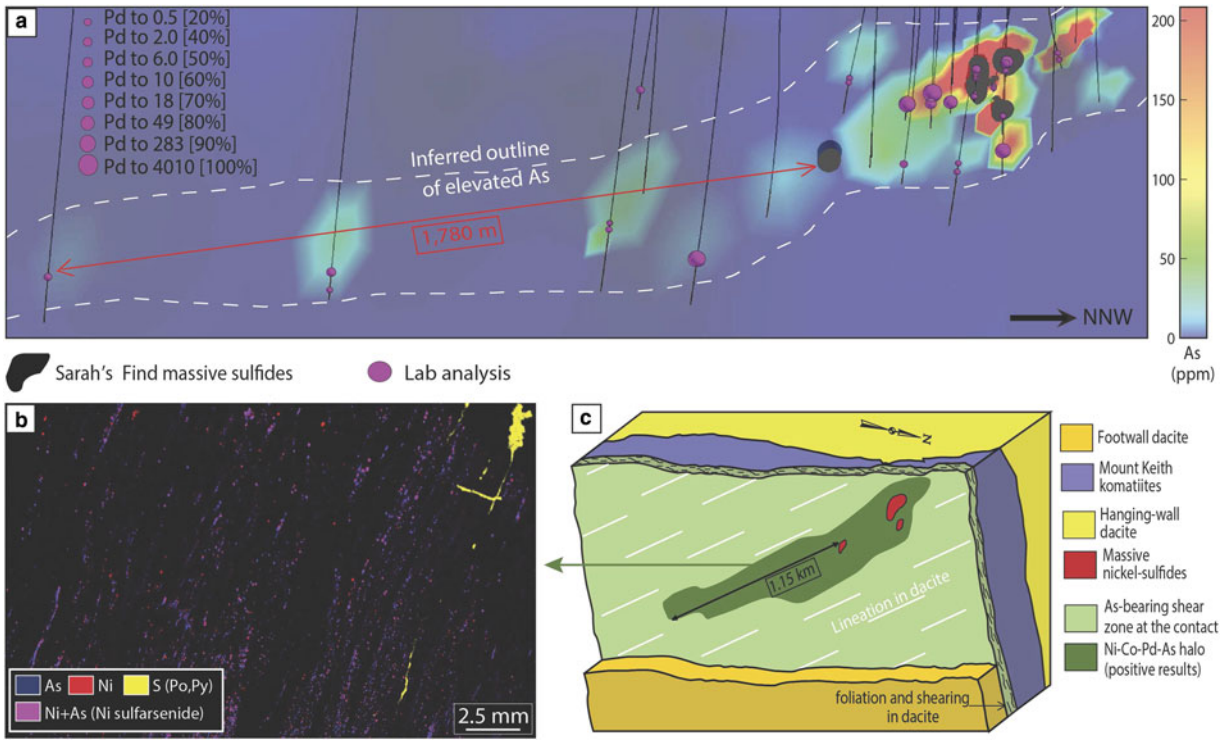

FIG. 7. Summary of results from the study of hydrothermal haloes around the Sarah's Find deposit, modified from Le Vaillant *et al.* (2016*b*). (*a*) 3D visualization of concentrations in Pd of all analysed samples, combined with a colour representation of the arsenic concentrations along the footwall contact between the Mount Keith komatiites and the Mount Keith dacite. (*b*) micro-XRF map of one of the sample containing nickel arsenides within the foliation in the dacite footwall. (*c*) Interpretative block model of the geochemical halo observed around the Sarah's Find ore body. Adapted from Le Vaillant *et al.* (2016*a*).

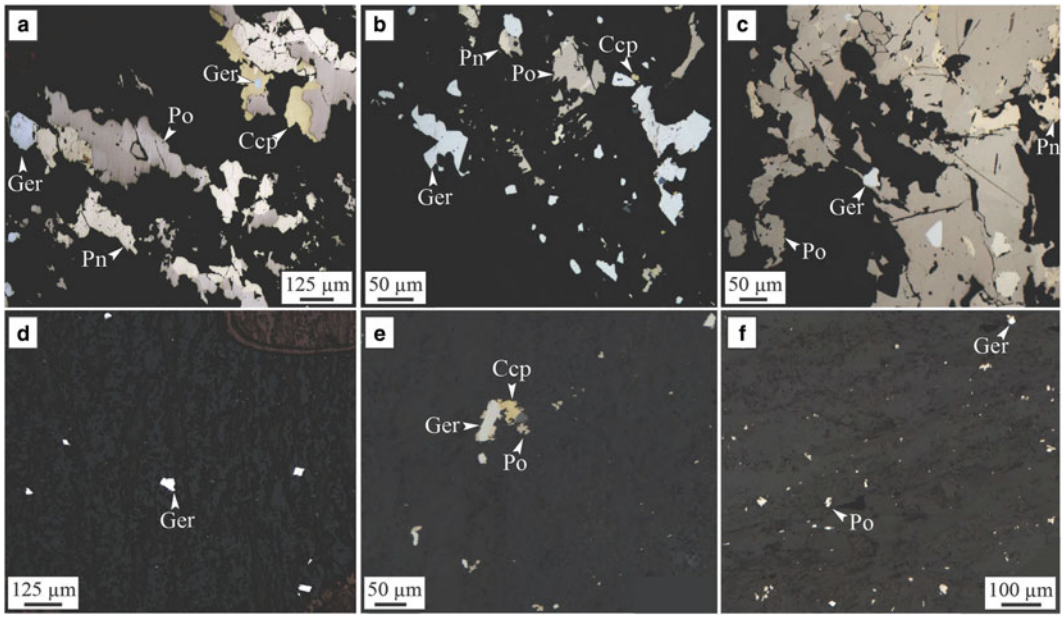

FIG. 8. Sarah's Find. Photomicrograph in reflected light of samples from the Sarah's Find nickel prospect. (*a*, *b* and *c*) show the assemblage present in area of the mineralization altered by As-rich fluids or where mechanically remobilized sulfides were altered by As-rich hydrothermal fluids ('Type 2'); (*d*, *e* and *f*) show the presence of hydrothermal arsenide grains ('Type 1') within the foliation of the dacite footwall, forming a halo around the mineralization. (*a*) Sample MKTD19-281A; (*b*) sample MKTD506-273A; (*c*) sample MKTD506-273B; (*d*) sample MKTD506-273C; (*e*) sample MKTD23-303A; and (*f*) sample MKTD23-303C. Ccp = chalcopyrite, Ger = gersdorffite, Pn = pentlandite and Po = pyrrhotite. From Le Vaillant *et al.* (2016*b*).

(2c) is characterized by the presence of patches/veins of calcite – dolomite – pyrrhotite – pentlandite – chalcopyrite – chlorite – gold ± ilmenite ± cobaltite ± biotite. Gold occurs in the core of the veins developed in this sub-stage along with pyrrhotite, pentlandite and cobaltite (Fig. 9). Within sub-stage 2c, Mn-rich (up to 1.5 wt.%) calcite cross-cuts euhedral to subhedral Mn-poor calcite blades; cobaltite and gold can occur in these Mn-rich calcite fractures.

Stage 2c arsenides (arsenopyrite, cobaltite, nickeline, maucherite ± gersdorffite) are up to several hundred micrometres in size and occur as clots surrounding amphiboles in chlorite-tremolite –

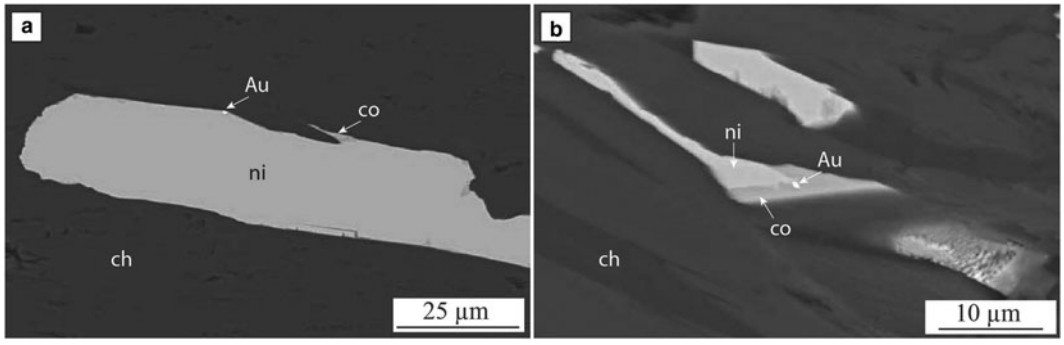

FIG. 9. Wattle Dam. Back-scatter electron image of the arsenides observed at the Wattle Dam gold deposit. (*a*) nickeline, chlorite, cobaltite and gold in altered komatiite ~100 m away from the main lode; (*b*) nickeline, chlorite, cobaltite and gold overprinting amphibole in altered komatiite ~50 m away from the main lode. Adapted from Walshe *et al.* (2014).

https://doi.org/10.1180/minmag.2017.081.100 Published online by Cambridge University Press

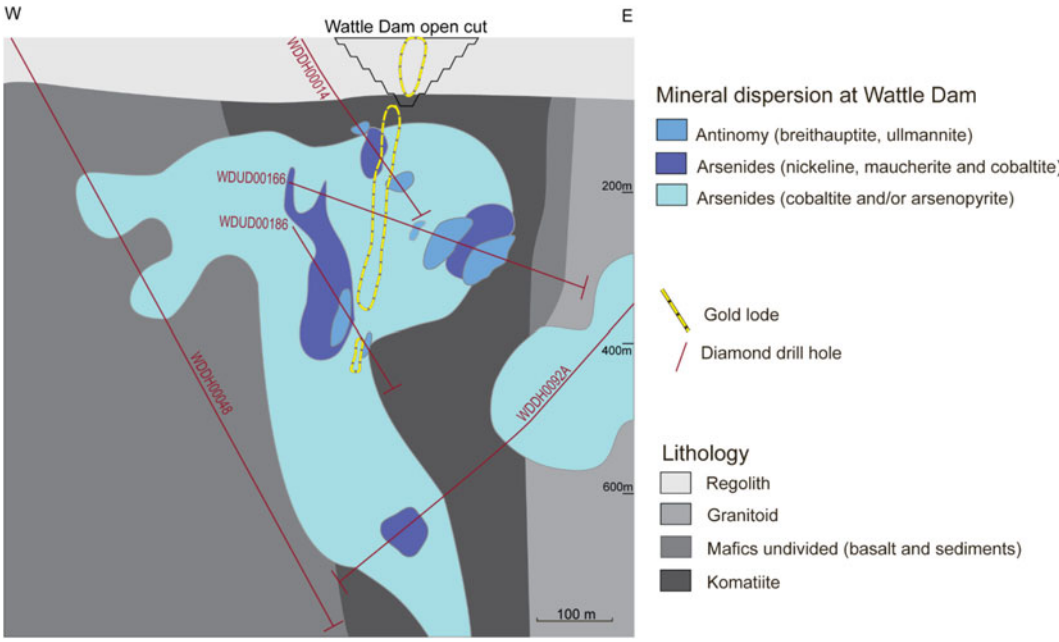

FIG. 10. Cross-section of alteration domains from the Wattle Dam deposit. The cross-section shows the location of the main lode. Alteration zones are based on the distribution of indicator minerals along drill holes that are shown in the illustration. Figure from Walshe *et al.* (2014).

carbonate altered komatiites within 100 m of the main lode. Stage 2c nickeline is rimmed by cobaltite (Fig. 9*a*) and/or gersdorffite. In a number of nickeline-rich samples, gold was identified as inclusions in cobaltite, which occurs along the margin of nickeline (Fig. 9*a*). Stage 2c gold was also identified along the margins of nickeline (Fig. 9*b*). The occurrence of gold inclusions in cobaltite and nickeline indicates a link between the timing of gold mineralization and arsenides at the Wattle Dam deposit. Graphite was also observed associated with arsenides. The presence of cobaltite or arsenopyrite in graphite with quartz and chlorite indicates that arsenides formed under reduced conditions.

At Wattle Dam, arsenides are distributed widely and can be found in komatiites near the main lode, and in basaltic rocks up to 400 m away from the main lode. An arsenide zone appears to extend laterally in the east and west direction away from the mineralized lode and beneath the main lode (Fig. 10).

The Mariners deposit: a magmatic nickel sulfide deposit with overprinting gold mineralization

The Mariners nickel deposit is, like the Miitel deposit, an Archean komatiite-hosted Ni–Cu–PGE deposit located on the eastern flank of the Widgiemooltha Dome (Seat *et al.*, 2004) within the Kalgoorlie Terrane (Swager, 1997), ~4 km south of Miitel (Fig. 1). Ore bodies are also located at the basal contact between the Widgiemooltha komatiites and the Mount Edwards basalt. One of the characteristics of the Mariners deposit is its unusually high concentration in arsenic and gold.

The geology of the Mariners deposit is described by Goodgame (1997): the primary ore trough plunges for at least 750 m NE at ~50° along the north-south striking bedding contact that dips 35–70°E. The trough is filled with mainly high-magnesium komatiitic olivine cumulates up to 100 m thick. The cumulates have been heavily altered to talc-dolomite-magnesite-anthophyllite-chlorite assemblages indicating substantial carbonate addition. Peak metamorphism is indicated by biotite-actinolite assemblages in mafic rocks along shears, and by tremolite-anthophyllite-talc-dolomite-bearing assemblages in ultramafic rocks. Retrograde alteration along D_3 shears is represented by the replacement of pentlandite ($(Fe, Ni)_9S_8$) by arsenic minerals, gersdorffite (NiAsS) and nickeline (NiAs), as well as replacement of biotite by quartz, plagioclase, carbonate and chlorite.

https://doi.org/10.1180/minmag.2017.081.100 Published online by Cambridge University Press

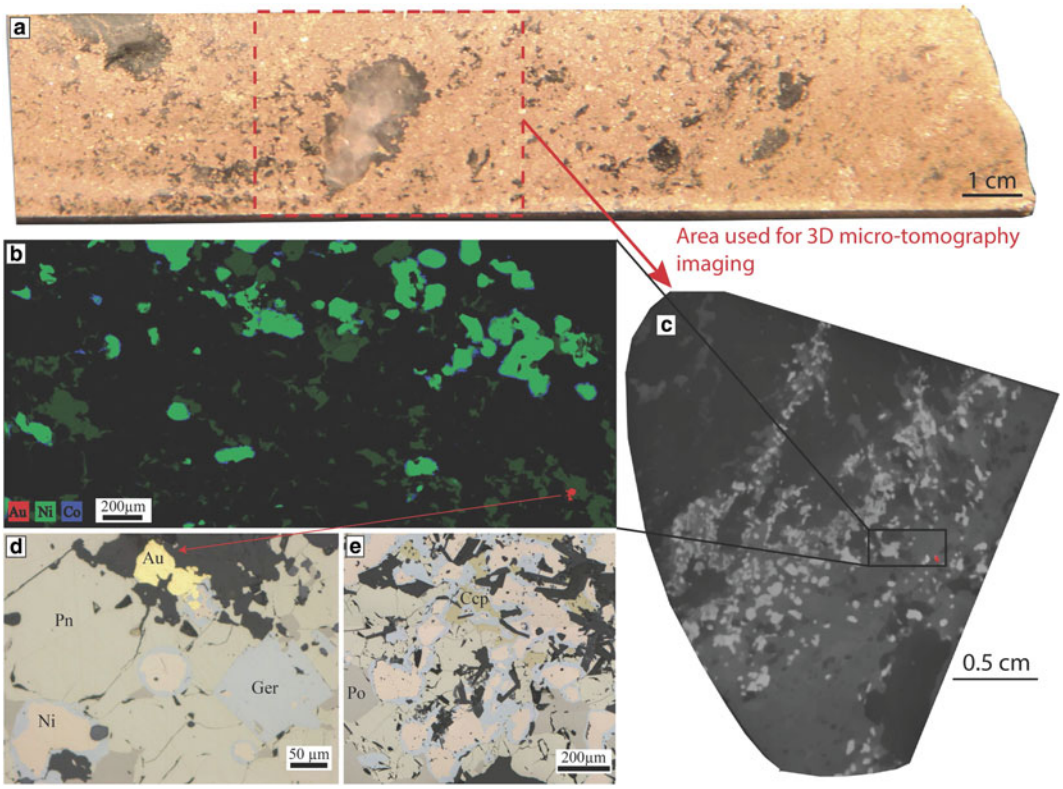

FIG. 11. Mariners. Nickel arsenides observed within the massive sulfides of the Mariners deposit. (*a*) Drill core photo of the sample used for this study, in red is the outline of the part of the sample that was used to collect a 3D micro-CT scan image. (*b*) Three elemental map showing the Ni-Co zoning of the arsenides at Mariners with a Ni-rich core and a Co-Fe rich rim. A gold grain is also visible in red. This map was produced using the data collected with either the Maia detector array on the X-ray fluorescence microscopy beamline, at the Australian Synchrotron in Melbourne. (*c*) Grey scale slice through the 3D micro CT scan of the sample that was used to locate gold grains for sectioning, gold grain also highlighted in red. (*d*,*e*) Photomicrographs in reflected light showing the nickel-arsenides with a nickeline core and a gersdorffite rim associated with the presence of gold. Au = gold, Ccp = chalcopyrite, Ger = gersdorffite, Ni = nickeline, Pn = pentlandite and Po = pyrrhotite.

This replacement by Ni arsenides is accompanied by enrichment in Au concentrations of the sulfides. Gold lodes are concentrated along D3 shear zones cross-cutting the magmatic nickel sulfides. In these areas of the ore body, arsenides are present in high concentrations. The sample used for our study was collected in one of these areas, in drill hole MRDH0230 at 414.07 m depth. This interval of the drill hole is particularly enriched in As and Au: 11.85 % Ni, 6150 ppb Au and 4.58% As (Fig. 11*a*). Arsenides present within the sample display a characteristic zoning with a core composed of nickeline and a rim composed of gersdorffite (Fig. 11*b*,*d*,*e*). Both cores and rims were analysed by LA-ICP-MS in this study.

Methodology: LA-ICP-MS

The concentrations of Ni, As, S and Fe were determined for each grain by electron microprobe on the Cameca SX50 instrument at CSIRO in Perth. Microprobe data were collected by wavelength dispersive spectrometry at an accelerating voltage of 15 Kv, beam current of 30 nA and counting times of 60 s per element (30 s peak 15 s background on each side).

The trace-element contents of arsenides were determined by LA-ICP-MS at LabMaTer, Université du Quebec à Chicoutimi (UQAC), Canada. The UQAC laser ablation system consists of an Agilent 7700x mass spectrometer with an Excimer 193 nm

https://doi.org/10.1180/minmag.2017.081.100 Published online by Cambridge University Press

Resonetics Resolution M-50 laser ablation probe. Samples plus reference material, Ni and Cu blanks were placed in the S155 Dual Volume Sample Cell together. The spectrum of the gas blank was collected for 20 s with the laser switched off to determine the background. Then line scans across the grains were carried out using a beam size of 15 to 44 µm, (depending on the grain size of the arsenides), a laser frequency of 15 Hz, a power of 0.5 mJ/cm^3 and a speed of lateral laser displacement of 5 µm/s. Each time the beam size was changed the reference materials and blanks were run to allow accurate calibration. An argon-helium gas mix was used as carrier gas. The material was then analysed using the mass spectrometer in time resolution mode using mass jumping and a dwell time of 10 ms/peak. The following isotopes were monitored: ^{29}Si, ^{33}S, ^{34}S, ^{57}Fe, ^{59}Co, ^{61}Ni, ^{65}Cu, ^{68}Zn, ^{75}As, ^{82}Se, ^{101}Ru, ^{103}Rh, ^{105}Pd, ^{107}Ag, ^{108}Pd, ^{121}Sb, ^{189}Os, ^{193}Ir, ^{195}Pt and ^{197}Au.

To calibrate for PGEs and Au at the Perservance deposit and Sarah's Find prospect, ^{34}S was used as the internal standard; in addition, the certified reference material po-727, which is a synthetic FeS doped with ~0.040 ppm of each of the PGEs and Au provided by the Memorial University of Newfoundland, was used. For the remaining elements we used the certified reference material MASS-1 a ZnCuFeS pressed powder pellet provided by the US Geological Survey and doped with 0.050–0.070 ppm of most chalcophile elements. Two in house reference materials, JB-MSS5 and UQAC-MSS-1, were used to monitor the accuracy of the calibration. JB-MSS5 is a synthetic FeS with 1 wt.% Ni, 0.020–0.065 ppm PGEs, Au, Ag, As, Bi, Sb, Se and Te provided by Prof. J. Brenan. UQAC-MSS1 consists of a synthetic $NiFeS_2$ provided by Dr. A. Peregoedova from McGill University, doped with ~0.002 ppm PGEs and Au.

This analytical protocol could not be used for the arsenide grains from the Mariners, Miitel and the Wattle Dam deposits because the S concentrations of the arsenides were either too variable or too low. Nickel was used as an internal standard for these arsenides; however, both po-727 and MASS-1 contain very little Ni and thus they could not be used for calibration. Therefore, we used MASS-3, an NiS pressed powder pellet provide by the US Geological Survey and doped with 50–70 ppm of most chalcophile elements to calibrate. UQAC-MSS-1 and JB-MSS-5 were used as monitors. Results obtained with the various monitors, analysed as unknown samples for each run to check data quality, are tabulated in Supplementary materials Tables S1, 2 and 3. These reference materials have been used in previous studies (Barnes *et al.*, 2008; Dare *et al.*, 2010*b*, 2011; Godel *et al.*, 2012; Le Vaillant *et al.*, 2015, 2016*b*).

^{101}Ru was corrected for ^{61}Ni interference by using a NiS blank bead; this correction is equivalent to ~0.001 to 0.0015 ppm in the arsenides. The amount of Cu interference on ^{103}Rh and ^{105}Pd from ^{63}Cu^{40}Ar and ^{65}Cu^{40}Ar, respectively, was determined by running a (CuFe)S_2 blank. The Cu corrections on Rh and Pd in the arsenides are <0.01 ppm; therefore, no correction for Cu interference was made. Data reduction was carried out using *Iolite* software (Paton *et al.*, 2011). Sulfur, As, Ni and Si were monitored to ensure that the minerals measured were arsenides. The presence inclusions of accessory minerals within the arsenides was monitored, and excluded from the time resolved spectrum before calculating the average signal. Their signals were not taken into account during the integration leading to the calculation of trace-elements concentrations in the mineral of interest.

Results

Arsenides from the Perseverance nickel deposit

Arsenides from Perseverance are all gersdorffite (NiAsS) with homogeneous compositions (average of 42.1 wt.% As, 21.1 wt.% S, 16.6 wt.% Ni, 8.3 wt.% Co and 8.4 wt.% Fe). These arsenides, which are the only purely magmatic arsenides in this study, have the highest PGE concentrations of all analysed arsenides, particularly in IPGEs (Os, Ir, Ru, Rh) (Figs 12, 13). Average concentrations of PGEs in arsenides at Perseverance are 100 ppm Pd, 132 ppm Pt, 20 ppm Os, 10 ppm Ir, 9 ppm Rh and 32 ppm Ru.

Arsenides from the Miitel nickel deposit

Arsenides from the Miitel deposit are all gersdorffite (NiAsS) with homogeneous As and S contents (averages of 49.1 wt.% As and 18.2 wt.% S) but varying Ni, Fe and Co contents due to substitutions (1.7–21.1 wt.% Co, 2.6–10.4 wt.% Fe and 10.4–28.6 wt.% Ni). Moreover, arsenides at Miitel have been separated in two 'types': the hydrothermal ones (type 1) and those that are due to local As-rich

https://doi.org/10.1180/minmag.2017.081.100 Published online by Cambridge University Press

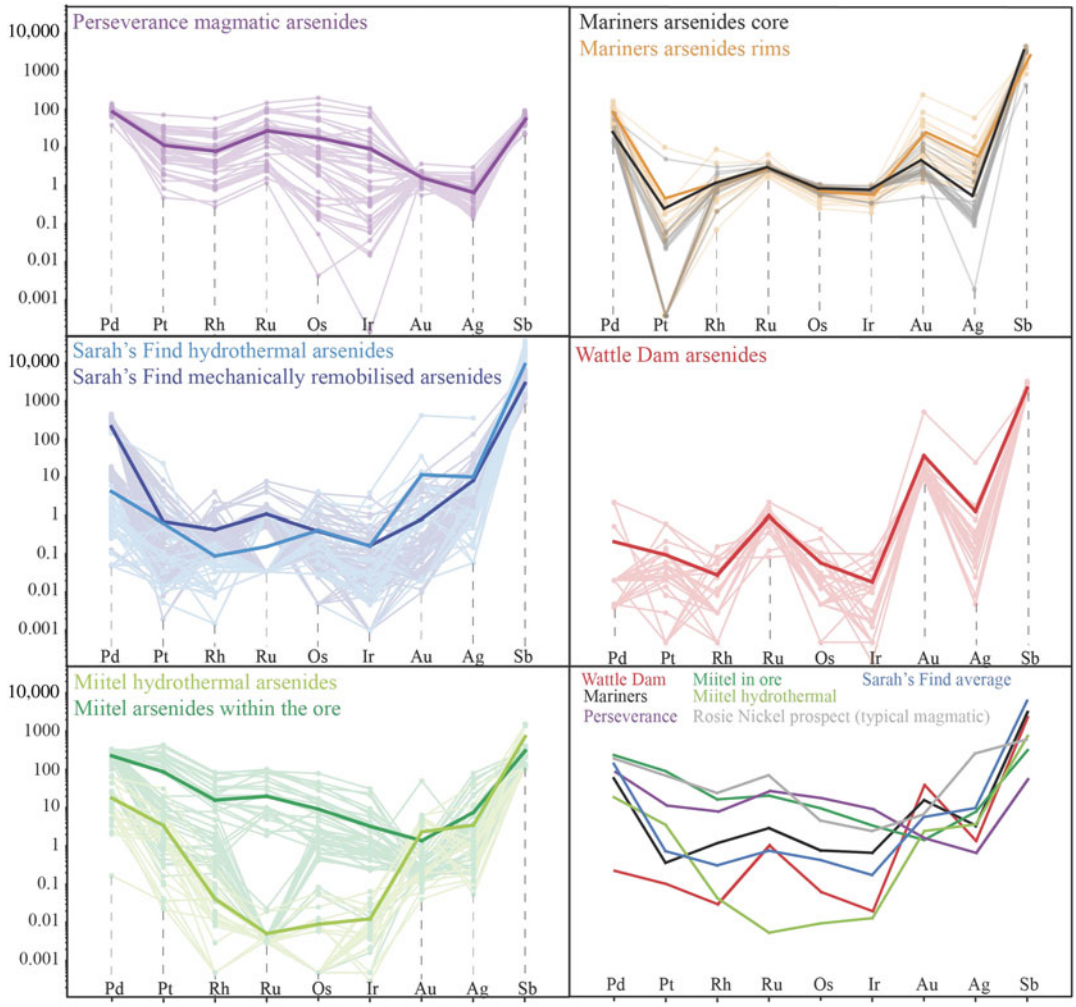

FIG. 12. Laser ablation trace-element analyses of arsenides from the various case studies. Data are plotted as mg/g with no normalization.

alteration of the massive sulfides (type 2; see description in Geological background). Gold, Sb and Ag contents of these two types are similar (1.4–4 ppm Au, 310–730 ppm Sb and 3.6–7.7 ppm Ag) but PGE contents vary a lot, with type 2 being more enriched in PGEs, particularly in IPGEs than type 1 (Figs 12, 13 and Table 1). IPGE concentrations of type 1 hydrothermal arsenides are the lowest compared to all arsenide studied here, whereas PGE contents of type 1 are the highest (with Perseverance) of all arsenides included in this study.

Arsenides from the Sarah's Find nickel prospect

Arsenides from the Sarah's Find prospect are also all gersdorffites (NiAsS) with homogeneous As and S contents averaging at 46 wt.% As and 19 wt.% S, but varying Ni, Fe and Co contents due to substitutions (1.3–16.54 wt.% Co, 3.7–8.2 wt.% Fe and 12.6–27 wt.% Ni) (Figs 12, 13). Also at Sarah's Find arsenides have been separated in two types: those that are purely hydrothermal (type 1) and those formed by local As-rich alteration of the

https://doi.org/10.1180/minmag.2017.081.100 Published online by Cambridge University Press

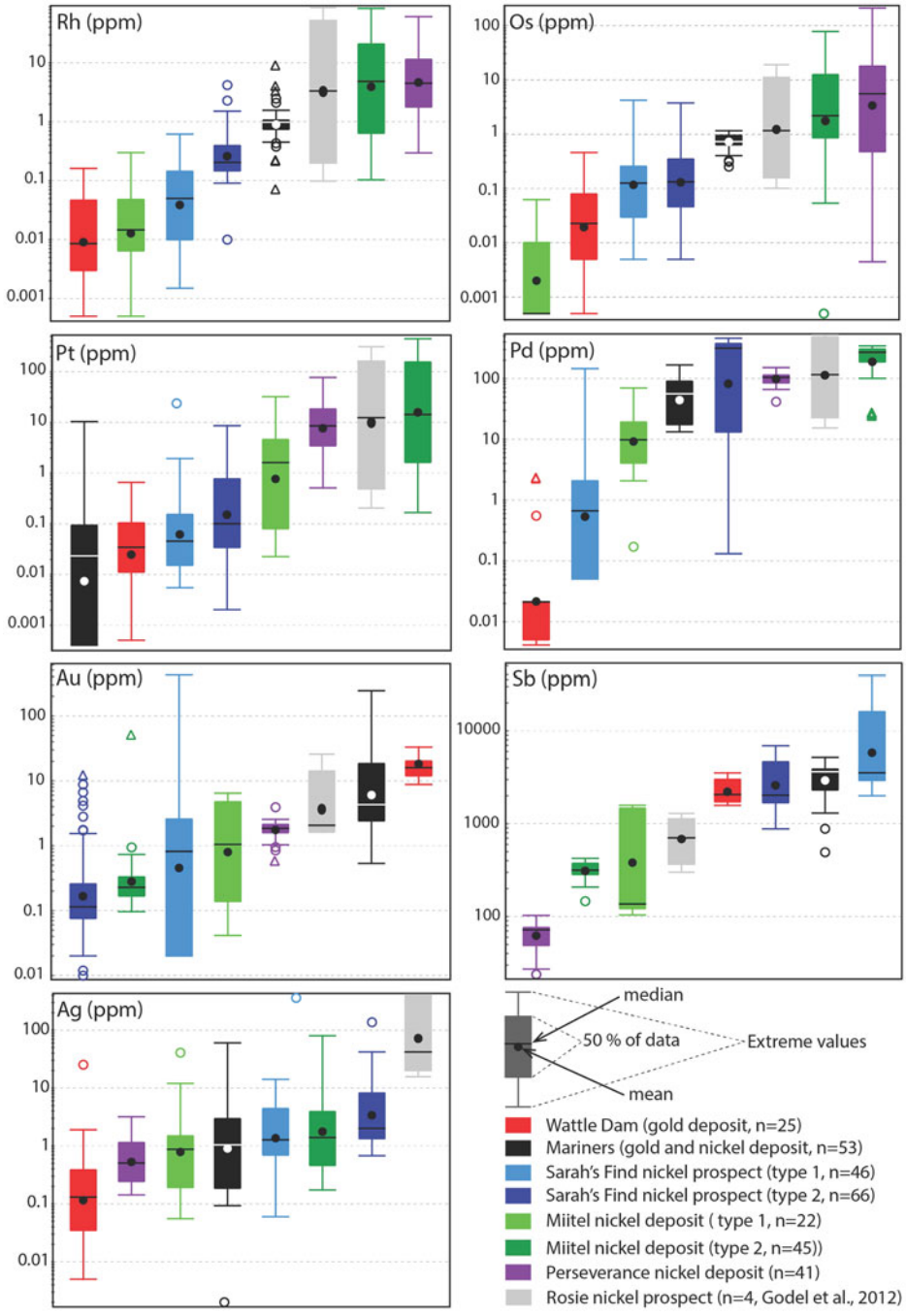

FIG. 13. Tukey box plots showing the distribution in PGEs, Au, Sb and Ag for the arsenides within the different case studies presented in this paper. Central box is the intra-quartile range, outlier points (circles) are further than 1.5 x (Q3-Q1) from the box, triangles further than 3 × (Q3-Q1), dot = mean, dash = median, whiskers are extreme values that are not outliers. For arsenides from the Sarah's Find and Miitel localities, 'Type 1' are hydrothermal arsenides whereas 'Type 2' are arsenides located within magmatic sulfides that have been altered by As-rich hydrothermal fluids.

https://doi.org/10.1180/minmag.2017.081.100 Published online by Cambridge University Press

TABLE 1. Representative compositions of arsenides from different localities.*

Mineral phase		*n*		As (wt%)	Co (wt%)	Fe (wt%)	Ni (wt%)	S (wt%)	^{107}Ag (ppm)	^{197}Au (ppm)	^{65}Cu (ppm)	^{193}Ir (ppm)	^{189}Os (ppm)	^{105}Pd (ppm)	^{195}Pt (ppm)	^{103}Rh (ppm)	^{101}Ru (ppm)	^{121}Sb (ppm)	^{82}Se (ppm)	^{118}Sn (ppm)
Wattle dam																				
NiAs	Hydro-thermal	25	AV	56.21	0.17	0.39	43.01	0.29	1.30	37.94	10.68	0.02	0.06	0.22	0.10	0.03	0.98	2248.99	16.50	0.39
			SD	1.94	0.11	0.20	1.91	0.11	5.01	104.45	20.48	0.03	0.10	0.62	0.17	0.04	0.49	652.26	8.09	0.32
Perseverance																				
NiFeCoAsS	Magmatic	41	AV	42.10	8.35	8.37	16.57	21.13	0.76	1.84	743.55	10.63	20.71	100.02	13.24	9.24	31.86	64.27	8.99	0.10
			SD	0.93	0.28	0.62	1.22	0.38	0.68	0.56	1872.90	23.85	42.10	21.60	14.79	11.62	36.20	18.71	0.96	0.10
Miitel (Le Vallant *et al.*, 2015)																				
NiFeCoAsS	Type 2	45	AV	48.23	7.89	4.63	22.53	18.81	7.69	1.41	335.97	3.33	9.38	230.55	87.82	16.07	20.12	310.34	84.49	0.37
			SD	0.69	4.27	0.31	3.95	0.26	16.54	7.49	1324.23	6.48	15.89	98.76	121.83	23.25	32.17	61.34	17.25	0.17
	Type 1	22	AV	49.14	2.66	6.14	24.96	18.21	3.59	2.39	1.94	0.01	0.01	18.28	3.48	0.04	0.01	730.27	111.87	0.19
			SD	1.36	0.51	3.32	3.41	0.88	8.92	2.44	4.58	0.02	0.02	21.63	6.72	0.07	0.00	685.42	52.29	0.12
Mariners																				
NiFeCoAsS	Rim	30	AV	44.92	2.62	2.00	30.85	19.49	5.41	23.30	5434.80	0.54	0.66	79.95	0.43	1.12	2.65	2442.58	104.44	1.61
			SD	0.14	0.66	0.51	0.97	0.20	11.07	46.06	27343.73	0.24	0.29	38.06	1.86	1.66	1.18	1119.54	60.46	3.91
NiAs	Core	22	AV	55.17	0.01	0.07	44.38	0.31	0.54	4.89	1906.61	0.80	0.85	24.32	0.01	1.08	3.00	3810.15	31.76	0.54
			SD	0.11	0.01	0.04	0.10	0.04	0.93	5.43	6807.15	0.12	0.18	20.17	0.02	0.44	0.19	308.80	21.95	0.68
Sarah's find (Le Vallant *et al.*, 2016)																				
NiFeCoAsS	Type 2	66	AV	45.21	8.61	7.08	19.44	19.39	8.37	0.83	9.03	0.17	0.40	215.57	0.73	0.45	1.11	2953.92	22.00	0.75
			SD	0.35	4.96	0.70	4.00	0.57	18.24	2.08	20.77	0.41	0.74	175.48	1.45	0.65	1.33	1673.38	13.33	2.12
	Type 1	46	AV	46.39	3.42	4.81	25.94	18.26	10.35	11.84	12.84	0.17	0.43	4.35	0.66	0.09	0.16	9245.38	53.55	3.96
			SD	0.84	0.51	0.50	0.95	0.28	52.83	62.08	24.82	0.63	0.87	21.13	3.44	0.12	0.37	9828.30	128.55	11.95
Beni Bousera (Pina *et al.*, 2013)																				
NiAs	Magmatic Ni	1	AV	45.05	0.47	0.27	52.65	0.24	1.32	33.93	4128.00	25.85	8.29	61.73	7.48	8.64	7.55	2999.00	40.00	
Dundonald beach (Hanley, 2007)																				
NiAs	Magmatic Ni	2	AV											52.50	167.50			1824.50		
Rosie (Godel *et al.*, 2012)																				
NiFeCoAsS	Magmatic Ni	43	AV									2.15	5.43	234.53	83.38	28.80	84.95	742.30		
Spotted Quoll (Prichard *et al.*, 2013)																				
NiFeCoAsS	magmatic Ni	9	AV	41.50	4.29		23.47			0.11		1.24	2.34	257.56	536.22	15.33	10.61	266.89		
Bhukia-jagpura (Deol *et al.*, 2012)																				
FeAsS	Gold	25	AV		0.73		0.10		0.14	1.38	263.62				0.04			73.68	27.62	0.19
Tanami gold (Cook *et al.*, 2013)																				
FeAsS	Gold	10	AV		0.02		0.04		4.01	73.70								136.40	15.80	

* Concentrations in majors (As, S, Ni, Fe, Co) are obtained by microprobes analyses - see Method section.
Concentrations in trace elements are obtained by LA-ICP-MS analyses - see Method section.
AV = average; SD = standard deviation; *n* = number of analyses

massive sulfides (type 2). Their compositional range is less than that observed at Miitel, but a difference can still be observed, with more elevated Au concentrations (average of 11.8 mg/g Au) and lower PGE concentrations (average concentrations of 4.3 ppm Pd, 0.6 ppm Pt, 4 ppm Os, 0.1 ppm Ir, 0.1 ppm Ru and 09 ppm Rh) in type 1 (hydrothermal) compared to type 2 (average concentrations of 0.8 ppm Au, 215 ppm Pd, 0.7 ppm Pt, 0.4 ppm Os, 0.2 ppm Ir, 1.1 ppm Ru and 0.4 ppm Rh). Compared to other arsenides studied in this project, arsenides from Sarah's Find seem to have average concentrations in PGEs and Au, but elevated concentrations in Sb (average of 5500 ppm Sb).

Arsenides from the Wattle Dam gold deposit

Arsenides from the Wattle Dam deposit were nickeline (NiAs) with the following average composition: 56.2 wt.% As, 43 wt.% Ni and trace amounts (<0.5 wt.%) of Co, Fe and S. These arsenides are enriched in Au, with an average of 0.017 ppm. Concentrations in platinum-group elements are low with an average of 6 ppm Pd, 1 ppm Pt, 5 ppm Ru, 1 ppm Os and Ir and Rh below 0.5 ppm. Concentrations in Sb are also fairly elevated, with an average of 2250 ppm (Table 1 and Fig. 12). When compared with all other arsenides within the study, the nickeline grains from the Wattle Dam deposit are the least enriched in Pd, Pt and Rh, and the most enriched in Au and PGEs (Fig. 12, Fig. 13).

Arsenides from the Mariners nickel and gold deposit

Arsenides from the Mariners deposit analysed within this study presented a characteristic zoning with a core of nickeline (NiAs), with average compositions of 55.1 wt.% As and 44.4 wt.% Ni and trace amounts of Co, Fe and S, and a rim of gersdorffite (NiAsS), with an average composition of 44.9 wt.% As, 30.8 wt.% Ni, 19.5 wt.% S, 2.6 wt.% Co and 2 wt.% Fe. The trace-element composition of the core and rims are very similar for IPGEs (5–8 ppm Ir, 6–8 ppm Os, 1.1 ppm Ru and 2.6–3 ppm Rh), as well as Sb contents, which are very elevated (2400–3800 ppm Sb; Table 1 and Fig. 12). Gold and PPGEs (Pt, Pd) seem to be a little more enriched in the rims than in the cores: 80 ppm Pd, 4 ppm Pt and 23 ppm Au average in rims compared to 24 ppm Pd, 0.1 ppm Pt and 4.9 ppm Au average in cores (Table 1 and Fig. 12). In general, compared to arsenides from other environments, arsenides within the Mariners deposit have elevated concentrations in Au and Sb, and average concentrations in PGEs (Fig. 12, Fig. 13).

Effects of mineral species and inter-element correlations

No systematic differences were observed in trace-element contents of Ni arsenide (nickeline, also called niccolite) compared with Ni–Co–Fe sulfarsenides in the only occurrence (Mariners) containing both species, with the exception of Se (median 100 ppm in sulfarsenides, 30 ppm in nickeline), Pd (80 and 20, respectively) and Pt (0.1 and 0.04, respectively). Nickeline rims at Mariners are not enriched in Au relative to sulfarsenides.

Considering only NiCoFe sulfarsenides, a number of weak inter-element correlations were noted between trace- and major-element contents over the entire set of occurrences (Fig. 14), although these can be attributed mostly to the paragenesis rather than the mineral chemistry. Sulfarsenides from Mariners are the most Ni rich (Table 1) and also the most Au rich (Fig. 14*c*). The Se contents of sulfarsenides increase with Ni content, but this trend is dominated by the low-Ni magmatic phases from Sarah's Find (Fig. 14*a*). The IPGEs Ir, Ru and Os along with Rh correlate strongly with one another over the entire sulfarsenide data set (Fig. 14*e*,*f*) but show no systematic relationship to Ni. Considering the magmatic arsenide phases from Perseverance alone, there are very strong positive correlations between Pt, Rh, Ru and somewhat less strong between Pt, Os and Ir. Other than these, no significant inter-element correlations are evident. Aside from a very weak correlation between Pd and Rh (Fig. 14*d*), dominated by the Perseverance data set, Pt and Pd are largely decoupled from the IPGEs and Rh.

Comparison between localities

Data on the composition of the various arsenides studied are plotted as mantle normalized averages in Fig. 15, and compared with literature data on known hydrothermal arsenides from Beni Bousera. Results can be summarized as follows: Purely magmatic nickel arsenides from Perseverance are enriched in PGEs compared to hydrothermal arsenides and also compared to concentrations obtained from the literature from the Rosie prospect

https://doi.org/10.1180/minmag.2017.081.100 Published online by Cambridge University Press

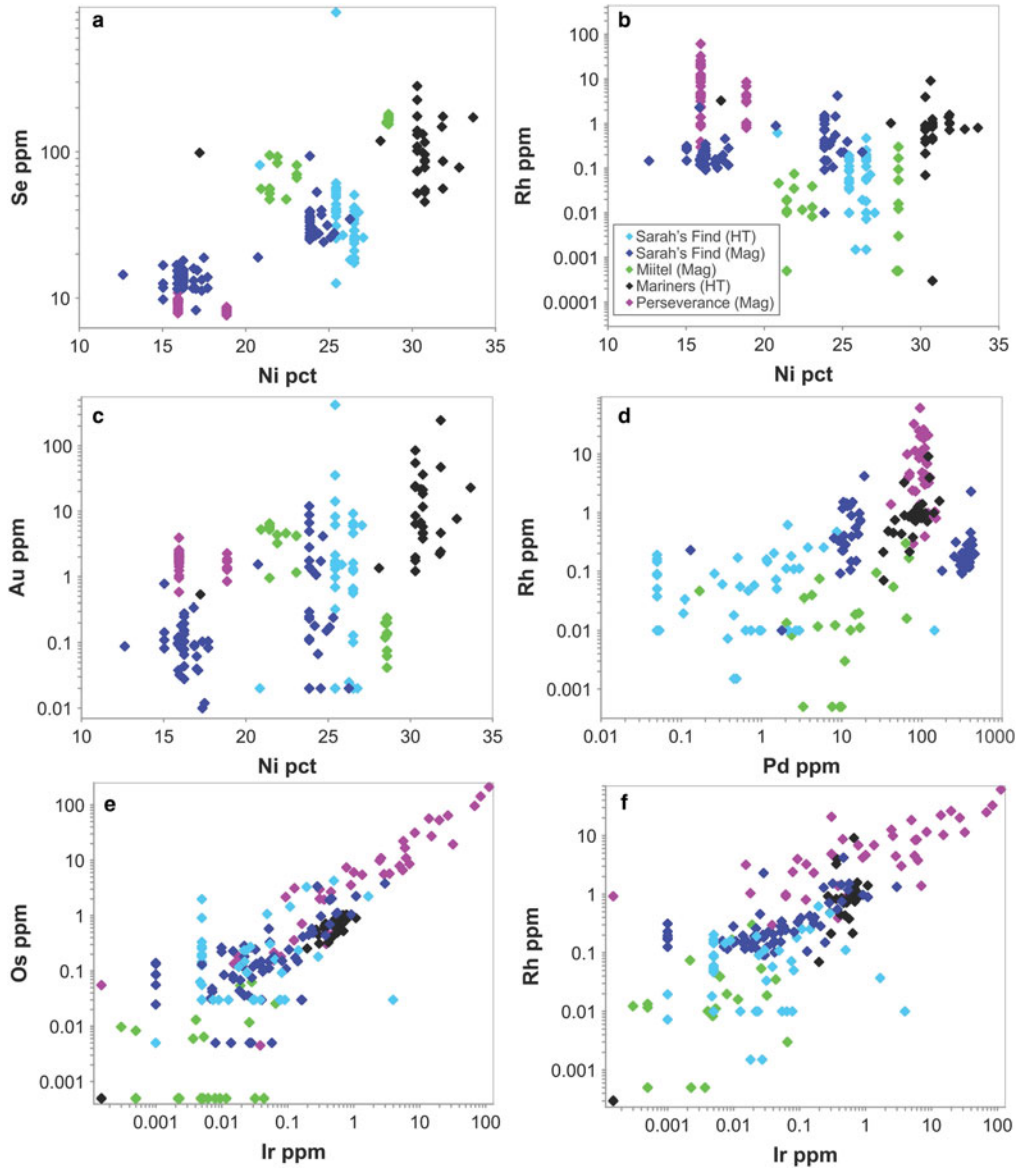

FIG. 14. Selected scatter plots showing inter-element concentrations in Ni–Co–Fe sulfarsenides from the various study sites. In the legend box, 'HT' stands for hydrothermal, and 'Mag' stands for magmatic.

and the Spotted Quoll deposit in Australia (Fig. 15). Concentrations in Au, Sb and Ag are more variable, lower than for Au deposits, but still higher than Au concentrations observed in hydrothermal Ni arsenides. Purely hydrothermal arsenides linked to Au mineralization on the contrary have low PGE concentrations compared to magmatic Ni arsenides (Wattle Dam deposit), but their Au concentrations are the highest, along with elevated Sb. Interestingly, Ag contents of the arsenides at Wattle Dam are very low.

Hydrothermal arsenides associated with Ni sulfide deposits generally have PGE concentrations that are more elevated than arsenides associated with Au deposits, but lower than magmatic arsenides, whereas their Au contents are lower

https://doi.org/10.1180/minmag.2017.081.100 Published online by Cambridge University Press

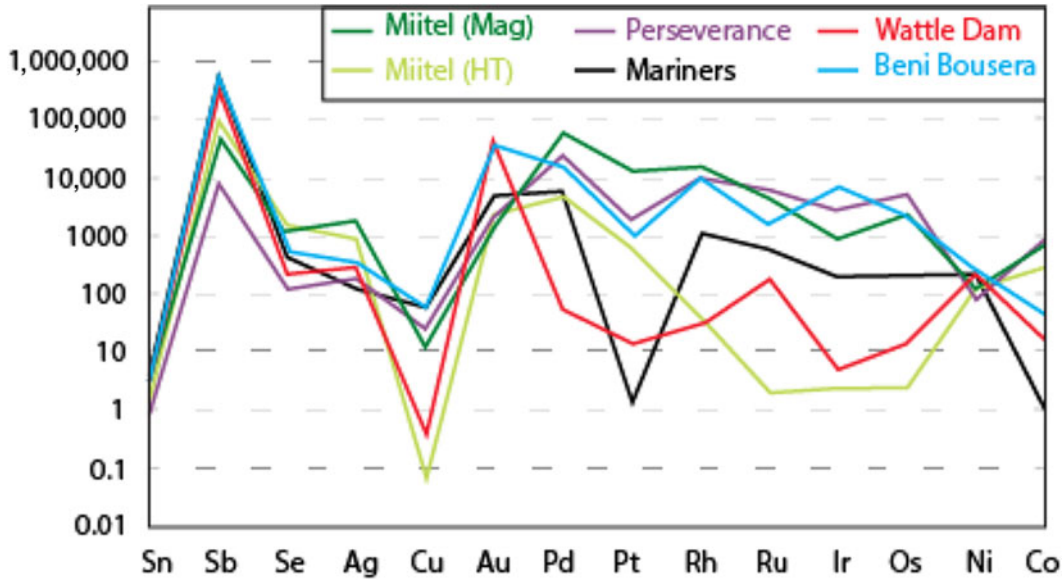

FIG. 15. Mantle normalized average element abundances for the various study areas, compared with data from Beni Bousera (Pina *et al.*, 2015). Element order (based on silicate melt compatibility) and mantle normalizing values from Lesher and Keays (2002).

than both magmatic and Au associated arsenides. However, these hydrothermal arsenides can be divided in two main categories. (1) Arsenides that crystallize directly from the As-rich hydrothermal fluids, away from the massive sulfides, observed within a secondary geochemical halo at Miitel and Sarah's Find (Type 1); and (2) arsenides that crystallized in place within the massive sulfides during alteration by the As-rich hydrothermal fluids such as the ones observed at Mariners where the fluids carry important amounts of Au, but also at Miitel within the massive sulfides (Type 2) and at Sarah's Find, where some have been mechanically remobilized along with the sulfides during deformation (type 2). Slightly different trace-element concentrations can be observed for these two categories of arsenides. Category 2 shows more elevated PGE concentrations than category 1, which displays higher Au contents, except for arsenides from the Mariners Ni–Au deposit which show very elevated Au concentrations, as expected.

Discussion

Processes controlling PGE and Au contents of arsenide phases

In the systems studied here, the source of PGEs and Ni is the mafic-ultramafic magma, whereas the source of Au is either the magma, material assimilated by the magma during emplacement, or the hydrothermal fluids affecting the system later. The crystallization of arsenides from the magmatic sulfide melt, with or without an intervening stage of formation of an immiscible arsenide liquid, is primarily controlled by the As content of the sulfides (Hanley, 2007; Helmy *et al.*, 2013*b*; Bai *et al.*, 2017; Canali *et al.*, 2017), which in turn is controlled by the amount of As assimilated into the magma during the ore forming process. Other factors such as timing of monosulfide solid-solution fractionation and saturation in PGE arsenide minerals are likely to play a major role in the final deposition of PGEs, introducing complexities that cannot be resolved with the present data set.

The Au content of these arsenides may depend on the amount of Au present within the assimilated crust material upon emplacement of the magma, but is also very likely to be modified by secondary processes such as sea-floor hydrothermal alteration or later regional hydrothermal overprinting. This additional complexity explains why Au contents of magmatic nickel arsenides (Perseverance, Rosie and Spotted Quoll) vary widely from one deposit to another. Experimental data on solubilities of PGEs in As-bearing fluids are lacking, but empirical observations on the association of PGEs with As in

https://doi.org/10.1180/minmag.2017.081.100 Published online by Cambridge University Press

hydrothermal settings imply that the solubility of PGEs in aqueous fluids is greatly enhanced by the presence of As-bearing ligands (see Le Vaillant *et al.*, 2015 and references therein). The composition of arsenides formed by hydrothermal fluids away from massive sulfides will depend on the composition of the fluids and the pressure and temperature conditions of deposition. Therefore, arsenides that form within an Au mineralized environment where no Ni-PGE enriched sulfides are present will be enriched in Au, but poor in PGEs, as observed at the Wattle Dam deposit. The fact that arsenides within hydrothermal haloes around Miitel and Sarah's Find contain PGEs implies that these elements were remobilized and transported by As-rich hydrothermal fluids. As expected, these arsenides contain more Pd and Pt compared to the other PGEs, which are less mobile in hydrothermal fluids.

Finally, the composition of arsenides within massive nickel sulfide ore bodies will depend on both the composition of the As-rich hydrothermal fluids and the composition of the altered sulfides. At Mariners, the fluids are inferred to have been enriched in Au, based on the presence of Au concentrations typical of hydrothermal lode Au deposits. Therefore, arsenides produced in this way contain high Au concentrations compared to the ones observed within the mineralization at Miitel and Sarah's Find, where no anomalous Au contents are observed. In contrast, sulfides at Miitel are very enriched in PGEs; therefore, arsenides produced within the mineralization through the process of alteration of As-rich hydrothermal fluids are also very rich in PGEs. Interestingly, arsenides at Mariners seem to have very low Pt concentrations compared to other PGEs. This could be explained by retention of Pt within its own platinum-group minerals (PGM).

Potential use of arsenides as indicator minerals

The first potential application lies in the interpretation of the petrogenesis of arsenide minerals and As-PGE anomalies associated with shear zones in greenstone terranes. The association of As with talc-carbonate alteration in shear zones is widespread in Archean greenstone terranes (e.g. Groves *et al.*, 2000). Where fluid-bearing shear zones intersect Au or Ni ores, potential exists for the mobilization of As and PGEs along the zones, as observed at Sarah's Find. The presence of PGE-enriched or Au-enriched arsenide minerals could be a distal footprint of the existence of mineralization upstream along the fluid flow path.

Secondly, arsenide minerals may well be sampled as part of heavy-mineral assemblages in environments of limited chemical weathering, such as in glacial till samples. PGE-enriched Ni–Co–Fe arsenides would be highly diagnostic indicators for magmatic Ni–Cu–PGE sulfide mineralization, and are likely to be much more abundant and detectable than PGMs themselves. Similarly, Au-enriched arsenides could serve as tracers for hydrothermal Au mineralization. Given that some arsenides, notably sperrylite, are known to be highly stable during weathering (Mota-e-Silva *et al.*, 2016), potential also exists for the survival of arsenide minerals in weathered terrains.

Conclusion

Variations are observed in the composition in PGEs and Au of Ni–Co sulfarsenides as a function of the environment in which the arsenides occur and the mineral phases they are associated with. At Miitel, primary Ni-sulfarsenides within magmatic massive sulfides are enriched in Pd and Pt, but also slightly enriched in IPGE (Ir, Os, Ru, Rh), whereas the Ni-sulfarsenides within the hydrothermal halo, concentrated within pervasively altered areas and quartz-carbonate veins, only contain Pd and Pt, in lower concentrations, and also often contain small amounts of Au. A similar observation is found at Sarah's Find, where the Ni–Co sulfarsenides associated with physical remobilization of the massive sulfides are enriched in all the PGEs (particularly Pd and Pt) whereas the Ni–Co sulfarsenides associated with hydrothermal remobilization from the massive sulfides, and concentrated in the foliation, are enriched in Pd and Pt only, in lower concentrations, and also contain small amounts of Au. Possible applications of this understanding would be: (1) the distal detection of shear hosted nickel sulfide or even Au ore bodies using the chemistry of As-bearing minerals, or anomalous arsenic bearing samples in shear zones; and (2) the use of PGE and or Au anomalous arsenide minerals as indicator minerals in glacial till samples.

Acknowledgements

Financial support for this research was provided by MERIWA (project #M413), BHP Billiton Nickel West, Mincor Resources NL and First Quantum

https://doi.org/10.1180/minmag.2017.081.100 Published online by Cambridge University Press

Minerals Ltd. The SIRF scholarship of the University of Western Australia and the MERIWA research grant are greatly appreciated. BHP Billiton Nickel West and Mincor Resources NL and are acknowledged for providing on site access and samples. Marco Fiorentini acknowledges support from the Australian Research Council through Linkage Project LP120100668 and the Future Fellowship Scheme (FT110100241). This is contribution 1024 from the ARC Centre of Excellence for Core to Crust Fluid Systems http://www.ccfs.mq.edu.au). The element maps presented in this manuscript were collected using the Maia Detector on the X-ray fluorescence microscopy beamline on the Australian Synchrotron in Clayton, Victoria. We acknowledge financial support for this facility from the Science and Industry Endowment Fund (SIEF). Finally, we would like to thank Danny Savard for help when collecting the LA-ICP-MS data at UQAC, as well as Malcom Roberts for his help when collecting microprobe data at the CMCA, Perth.

Supplementary material

To view supplementary material for this article, please visit https://doi.org/10.1180/minmag.2017.081.100

References

Ahmed, A.H., Arai, S. and Ikenne, M. (2009) Mineralogy and Paragenesis of the Co-Ni Arsenide Ores of Bou Azzer, Anti-Atlas, Morocco. *Economic Geology*, **104**, 249–266.

Bagheri, H., Moore, F. and Alderton, D.H.M. (2007) Cu-Ni-Co-As (U) mineralization in the Anarak area of central Iran: *Journal of Asian Earth Sciences*, **29**, 651–665.

Bai, L.P., Barnes, S.J. and Baker, D.R. (2017) Sperrylite saturation in magmatic sulfide melts: Implications for formation of PGE-bearing arsenides and sulfarsenides. *American Mineralogist*, **102**, 966–974.

Barnes, S.-J., Prichard, H., Cox, R., Fisher, P. and Godel, B. (2008) The location of the chalcophile and siderophile elements in platinum-group element ore deposits (a textural, microbeam and whole rock geochemical study): Implications for the formation of the deposits. *Chemical Geology*, **248**, 295–317.

Barnes, S.J., Fiorentini, M.L., Duuring, P., Grguric, B.A. and Perring, C.S. (2011) The Perseverance and Mount Keith Ni deposits of the Agnew-Wiluna Belt, Yilgarn Craton, Western Australia. *Reviews in Economic Geology*, **17**, 51–88.

Barnes, S.J., Fisher, L.A., Godel, B., Maier, W.D., Paterson, D., Howard, D.L., Ryan, C.G. and Laird, J. S. (2016) Primary cumulus platinum minerals in the Monts de Cristal Complex, Gabon: magmatic microenvironments inferred from high-resolution x-ray fluorescence microscopy. *Contributions to Mineralogy and Petrology*, **171**, 1285–1308.

Barnes, S.J., Gole, M.J. and Hill, R.E.T. (1988*a*) The Agnew Nickel Deposit, Western Australia: Part I. Structure and Stratigraphy. *Economic Geology*, **83**, 524–536.

Barnes, S.J., Gole, M.J. and Hill, R.E.T. (1988*b*) The Agnew nickel deposit, Western Australia: Part II. Sulfide geochemistry, with emphasis on the platinum-group elements. *Economic Geology*, **83**, 537–550.

Barnes, S.J. and Hill, R.E.T. (2000) Metamorphism of komatiite hosted nickel sulfide deposits. Pp. 203–216 in: *Metamorphosed and Metamorphogenic Ore Deposits* (P.G. Spry, B. Marshall and F.M. Vokes, editors). Reviews in Economic Geology, **11**. Society of Economic Geologists, Boulder, USA.

Canali, A.C., Brenan, J.M. and Sullivan, N.A. (2017) Solubility of platinum-arsenide melt and sperrylite in synthetic basalt at 0.1 MPa and 1200°C with implications for arsenic speciation and platinum sequestration in mafic igneous systems. *Geochimica et Cosmochimica Acta*, **216**, 153–168.

Caruso, S., Fiorentini, M.L., Moroni, M., Martin, L. (2017) Evidence of magmatic degassing in Archean komatiites: insights from the Wannaway nickel-sulfide deposit, Western Australia. *Earth and Planetary Science Letters*, **479C**, 252–262.

Cassidy, K.F., Champion, D.C., Krapez, B., Barley, M.E., Brown, S.J.A., Blewett, R.S., Groenewald, P.B. and Tyler, I.M. (2006) *A revised geological framework for the Yilgarn Craton, Western Australia*. Western Australia Geological Survey, **8**.

Cloutier, J., Walshe, J., Hough, R. and Bath, A. (2011) *Paragenesis, hyperspectral and stable isotope relationships in regards to gold mineralization and implications for gold exploration at the Wattle Dam deposit*. MERIWA M410 project interim report, MRIWA, Perth, Australia, pp.14.

Cloutier, J., Walshe, J.L., Hough, R., Bath, A. and Hutchison, R. (2012) Unravelling the paragenesis at one of Australia's highest-grade gold deposits. *Mineralogical Magazine*, **76**, 1582.

Cook, N.J. and Chryssoulis, S.L. (1990) Concentrations of invisible gold in the common sulfides. *Canadian Mineralogist*, **28**, 1–16.

Cook, N.J., Ciobanu, C.L., Meria, D., Silcock, D. and Wade, B. (2013) Arsenopyrite-pyrite association in an orogenic gold ore: tracing mineralization history from textures and trace elements. *Economic Geology*, **108**, 1273–1283.

Dare, S.A., Barnes, S.-J., Prichard, H.M. and Fisher, P.C. (2010*a*) The timing and formation of platinum-group minerals from the Creighton Ni-Cu-platinum-group element sulfide deposit, Sudbury, Canada: early

crystallization of PGE-rich sulfarsenides. *Economic Geology*, **105**, 1071–1096.

Dare, S.A.S., Barnes, S.-J. and Prichard, H. (2010*b*), The distribution of platinum group elements (PGE) and other chalcophile elements among sulfides from the Creighton Ni–Cu–PGE sulfide deposit, Sudbury, Canada, and the origin of palladium in pentlandite: *Mineralium Deposita*, **45**, 765–793.

Dare, S.A.S., Barnes, S.-J., Prichard, H. and Fisher, P. (2011) Chalcophile and platinum-group element (PGE) concentrations in the sulfide minerals from the McCreedy East deposit, Sudbury, Canada, and the origin of PGE in pyrite. *Mineralium Deposita*, **46**, 381–407.

De Almeida, C.M., Olivo, G.R. and de-Carvalho, S.G. (2007) The Ni-Cu-PGE sulfide ores of the komatiite-hosted Fortaleza de Minas deposit, Brazil: Evidence of hydrothermal remobilization. *Canadian Mineralogist*, **45**, 751–773.

Deol, S., Deb, M., Large, R.R. and Gilbert, S. (2012) LA-ICPMS and EPMA studies of pyrite, arsenopyrite and loellingite from the Bhukia-Jagpura gold prospect, southern Rajasthan, India: Implications for ore genesis and gold remobilization. *Chemical Geology*, **326**, 72–87.

Diragitch, A.A. (2014) *Geological Controls on the Distribution of Arsenic in the Perseverance Nickel Deposit*. Curtin University, Leinster, USA.

Eilu, P. and Groves, D.I. (2001) Primary alteration and geochemical dispersion haloes of Archaean orogenic gold deposits in the Yilgarn Craton: the pre-weathering scenario. *Geochemistry: Exploration, Environment, Analysis*, **1**, 183–200.

Fiorentini, M.L., Rosengren, N., Beresford, S.W., Grguric, B. and Barley, M.E. (2007) Controls on the emplacement and genesis of the MKD5 and Sarah's Find Ni–Cu–PGE deposits, Mount Keith, Agnew–Wiluna Greenstone Belt, Western Australia. *Mineralium Deposita*, **42**, 847–877.

Gervilla, F., Leblanc, M., Torres-Ruiz, J. and Hach-Ali, P. F. (1996) Immiscibility between arsenide and sulfide melts: A mechanism for the concentration of noble metals. *Canadian Mineralogist*, **34**, 485–502.

Gervilla, F., Papunen, H., Kojonen, K. and Johanson, B. (1998) Platinum-, palladium- and gold-rich arsenide ores from the Kylmakoski Ni-Cu deposit (Vammala Nickel Belt, SW Finland). *Mineralogy and Petrology*, **64**, 163–185.

Gervilla, F., Sanchez-Anguita, A., Acevedo, R.D., Hach-Ali, P.F. and Paniagua, A. (1997) Platinum-group element sulpharsenides and Pd bismuthotellurides in the metamorphosed Ni-Cu deposit at Las Aguilas (Province of San Luis, Argentina). *Mineralogical Magazine*, **61**, 861–877.

Godel, B., Gondzalez-Alvarez, I., Barnes, S.J., Barnes, S.-J., Parker, P. and Day, J. (2012) Sulfides and sulfarsenides from the Rosie Nickel Prospect, Duketon Greenstone Belt, Western Australia. *Economic Geology*, **107**, 275–294.

Goldfarb, R., Baker, T., Dube, B., Groves, D.I., Hart, C.J. R. and Gosselin, P. (2005) Distribution, character and genesis of gold deposits in metamorphic terranes. *One Hundredth Anniversary Volume* (J.W. Hedenquist, J.F. H. Thompson, R.J. Goldfarb and J.P. Richards, editors). Society of Economic Geologists.

Goodgame, V.R. (1997) *The Distribution and Origin of Arsenic and Platinum Group Element Mineralisation in the Mariners Nickel Deposit, Widgiemooltha, Western Australia*. Thesis, University of Oregon, USA.

Goodz, M.D. (1986) Sulphur-isotope geochemistry of silver-sulpharsenide vein mineralization, Cobalt, Ontario. *Canadian Journal of Earth Sciences*, **23**, 1551–1567.

Groves, D.I., Goldfarb, R.J., Knox-Robinson, C.M., Ojala, J., Gardoll, S., Yun, G.Y. and Holyland, P. (2000) Late-kinematic timing of orogenic gold deposits and significance for computer-based exploration techniques with emphasis on the Yilgarn Block, Western Australia. *Ore Geology Reviews*, **17**, 1–38.

Hanley, J.J. (2007) The role of arsenic-rich melts and mineral phases in the development of high-grade Pt-Pd mineralization within komatiite-associated magmatic Ni-Cu sulfide horizons at Dundonald Beach South, Abitibi Subprovince, Ontario, Canada. *Economic Geology*, **102**, 305–317.

Hayward, N. (1988) *Geology of the Widgiemooltha area and exploration progress to February* 1988. WMC Resources Internal Report K/3099, p. 144.

Helmy, H.M., Ballhaus, C., Wohlgemuth-Ueberwasser, C., Fonseca, R.O.C. and Laurenz, V. (2010) Partitioning of Se, As, Sb, Te and Bi between monosulfide solid solution and sulfide melt - Application to magmatic sulfide deposits. *Geochimica et Cosmochimica Acta*, **74**, 6174–6179.

Helmy, H.M., Ballhaus, C., Fonseca, R.O.C., Wirth, R., Nagel, T. and Tredoux, M. (2013*a*) Noble metal nanoclusters and nanoparticles precede mineral formation in magmatic sulfide melts. *Nature Communications*, **4**, article 2405.

Helmy, H.M., Ballhaus, C., Fonseca, R.O.C. and Nagel, T. J. (2013*b*) Fractionation of platinum, palladium, nickel, and copper in sulfide-arsenide systems at magmatic temperature. *Contributions to Mineralogy and Petrology*, **166**, 1725–1737.

Hem, S.R., Makovicky, E. and Gervilla, F. (2001) Compositional trends in Fe, Co and Ni sulfarsenides and their crystal-chemical implication: Results from the Arroyo de la Cueva deposits, Ronda Peridotite, Southern Spain. *Canadian Mineralogist*, **39**, 831–853.

Hutchison, R. (2011) Geology and definition of the Wattle Dam coarse gold deposit. *The AusIMM Bulletin*, **4**, 49–55.

https://doi.org/10.1180/minmag.2017.081.100 Published online by Cambridge University Press

Keays, R.R. and Jowitt, S.M. (2013) The Avebury Ni deposit, Tasmania; a case study of an unconventional nickel deposit. *Ore Geology Reviews*, **52**, 4–17.

Ketris, M. and Yudovich, Ya.E. (2009) Estimations of Clarkes for Carbonaceous biolithes: World averages for trace element contents in black shales and coals. *International Journal Coal Geology*, **78**, 135–148.

Le Vaillant, M., Barnes, S.J., Fiorentini, M.L., Miller, J., McCuaig, T.C. and Muccilli, P. (2015) A hydrothermal Ni-As-PGE geochemical halo around the Miitel komatiite-hosted nickel sulfide deposit, Yilgarn Craton, Western Australia. *Economic Geology*, **110**, 505–530.

Le Vaillant, M., Fiorentini, M.L. and Barnes, S.J. (2016*a*) Review of lithogeochemical exploration tools for komatiite-hosted Ni-Cu-(PGE) deposits: *Journal of Geochemical Exploration*, **168**, 1–19.

Le Vaillant, M., Saleem, A., Barnes, S.J., Fiorentini, M.L., Miller, J., Beresford, S. and Perring, C. (2016*b*) Hydrothermal remobilisation around a deformed and remobilised komatiite-hosted Ni-Cu-(PGE) deposit, Sarah's Find, Agnew Wiluna greenstone belt, Yilgarn Craton, Western Australia. *Mineralium Deposita*, **51**, 369–388.

Leblanc, M. and Fisher, W. (1990) Gold and platinum group element in cobalt-arsenide ores: hydrothermal concentration from a serpentinite source-rock (Bou Azzer, Morocco). *Mineralogy and Petrology*, **42**, 197–209.

Lesher, C.M. and Keays, R.R. (2002) Komatiite-associated Ni-Cu-PGE deposits: geology, mineralogy, geochemistry and genesis. Pp. 579–617 in: *The Geology, Geochemistry Mineralogy and Mineral Beneficiation of Platinum Group Elements* (L.J. Cabri, editor). Canadian Institute of Mining Metallurgy and Petroleum Special Volume **54**.

Locmelis, M., Fiorentini, M.L., Barnes, S.J. and Pearson, N.J. (2013) Ruthenium variation in chromite from komatiites and komatiitic basalts – a potential mineralogical indicator for nickel sulfide mineralization. *Economic Geology*, **108**, 355–364.

McQueen, K.G. (1981) Volcanic-associated nickel deposits from around the Widgiemooltha Dome, Western Australia. *Economic Geology*, **76**, 1417–1443.

McQueen, K.G. (1987) Deformation and remobilization in some Western Australian nickel ores. *Ore Geology Reviews*, **2**, 269–286.

Moroni, M., Caruso, S., Barnes, S.J. and Fiorentini, M.L. (2017) Primary stratigraphic controls on ore mineral assemblages in the Wannaway komatiite-hosted nickel-sulfide deposit, Kambalda camp, Western Australia. *Ore Geology Reviews*, **90**, 634–666.

Mota-e-Silva, J., Prichard, H.M., Suarez, S., Ferreira Filho, C.F. and Fisher, P.C. (2016) Supergene alteration of platinum-group minerals and the formation of Pd-Cu-O and Pd-I-O compounds in the Limoeiro Ni-Cu-(PGE) deposit, Brazil. *Canadian Mineralogist*, **54**, 755–778.

Paton, C., Hellstrom, J., Paul, B., Woodhead, J. and Hergt, J. (2011) Iolite: Freeware for the visualisation and processing of mass spectrometric data. *Journal of Analytical Atomic Spectrometry*, **26**, 2508–2518.

Perring, C.S. (2015) A 3-D Geological and structural synthesis of the Leinster Area of the Agnew-Wiluna Belt, Yilgarn Craton, Western Australia, with special reference to the volcanological setting of komatiite-associated nickel sulfide deposits. *Economic Geology*, **110**, 469–503.

Pina, R., Gervilla, F., Barnes, S.-J., Ortega, L. and Lunar, R. (2013) Partition coefficients of platinum group and chalcophile elements between arsenide and sulfide phases as determined in the Beni Bousera Cr-Ni mineralization (North Morocco). *Economic Geology*, **108**, 935–951.

Pina, R., Gervilla, F., Barnes, S.J., Ortega, L. and Lunar, R. (2015) Liquid immiscibility between arsenide and sulfide melts; evidence from a LA-ICP-MS study in magmatic deposits at Serrania de Ronda (Spain). *Mineralium Deposita*, **50**, 265–279.

Prichard, H.M., Fisher, P.C., McDonald, I., Knight, R.D., Sharp, D.R. and Williams, J.P. (2013) The Distribution of PGE and the role of arsenic as a collector of PGE in the Spotted Quoll nickel ore deposit in the Forrestania Greenstone Belt, Western Australia. *Economic Geology and the bulletin of the Society of Economic Geologists*, **108**, 1903–1921.

Samalens, N., Barnes, S.-J. and Sawyer, E.J. (2016) The role of black shales as a source of sulfur and semimetals in magmatic nickel-copper deposits: Example from the Partridge River Intrusion, Duluth Complex, Minnesota, USA. *Ore Geology Reviews*. http://dx.doi.org/10.1016/j.oregeorev.2016.09.030

Sampson, E. and Hriskevich, M.E. (1957) Cobalt-arsenic minerals associated with aplites, at Cobalt, Ontario. *Economic Geology and the bulletin of the Society of Economic Geologists*, **52**, 60–75.

Seat, Z., Stone, W.E., Mapleson, D.B. and Daddow, B.C. (2004) Tenor variation within komatiite-associated nickel sulfide deposits: insights from the Wannaway Deposit, Widgiemooltha Dome, Western Australia. *Mineralogy and Petrology*, **82**, 317–339.

Swager, C.P. (1997) Tectono-stratigraphy of the late Archaean greenstone terranes in the southern Eastern Goldfields, Western Australia. *Precambrian Research*, **83**, 11–42.

Szentpeteri, K., Watkinson, D.H., Molnar, F. and Jones, P.C. (2002) Platinum-group elements-Co-Ni-Fe sulfarsenides and mineral paragenesis in Cu-Ni-platinum-group element deposits, Copper Cliff North Area, Sudbury, Canada. *Economic Geology*, **97**, 1459–1470.

Walshe, J.L., Bath, A.B., Cloutier, J. and Hough, R.M. (2014) *High grade Au deposits: processes to prediction, Report 145*. Geological Survey of Western Australia, **183**.

https://doi.org/10.1180/minmag.2017.081.100 Published online by Cambridge University Press